JOURNAL OF VIROLOGY, Sept. 2008, p. 8629–8646 Vol. 82, No. 17
0022-538X/08/$08.00+0 doi:10.1128/JVI.00616-08

Linker Histones Are Mobilized during Infection with Herpes Simplex Virus Type 1▽

Kristen L. Conn,[1] Michael J. Hendzel,[2] and Luis M. Schang[1,3]*

Departments of Biochemistry,[1] Experimental Oncology,[2] and Medical Microbiology and Immunology,[3] University of Alberta, Edmonton, Alberta, Canada

Received 19 March 2008/Accepted 13 June 2008

Histones interact with herpes simplex virus type 1 (HSV-1) genomes and localize to replication compartments early during infections. However, HSV-1 genomes do not interact with histones in virions and are deposited in nuclear domains devoid of histones. Moreover, late viral replication compartments are also devoid of histones. The processes whereby histones come to interact with HSV-1 genomes, to be later displaced, remain unknown. However, they would involve the early movement of histones to the domains containing HSV-1 genomes and the later movement away from them. Histones unbind from chromatin, diffuse through the nucleoplasm, and rebind at different sites. Such mobility is upregulated by, for example, phosphorylation or acetylation. We evaluated whether HSV-1 infection modulates histone mobility, using fluorescence recovery after photobleaching. All somatic H1 variants were mobilized to different degrees. H1.2, the most mobilized, was mobilized at 4 h and further so at 7 h after infection, resulting in increases in its "free" pools. H1.2 was mobilized to a "basal" degree under conditions of little to no HSV-1 protein expression. This basal mobilization required nuclear native HSV-1 genomes but was independent of HSV-1 proteins and most likely due to cellular responses. Mobilization above this basal degree, and increases in H1.2 free pools, however, depended on immediate-early or early HSV-1 proteins, but not on HSV-1 genome replication or late proteins. Linker histone mobilization is a novel consequence of cell-virus interactions, which is consistent with the dynamic interactions between histones and HSV-1 genomes during lytic infection; it may also participate in the regulation of viral gene expression.

Herpes simplex virus type 1 (HSV-1) is a nuclear replicating DNA virus that undergoes latent or lytic infections in neurons or epithelial cells, respectively. The infecting viral genomes are delivered to nuclear domains adjacent to ND10s, domains which are devoid of cellular chromatin (2, 20, 33). Lytic HSV-1 genomes then replicate in these domains, forming small replication compartments. The compartments grow and coalesce into large replication compartments, which later occupy large nuclear domains (31, 56, 61). Infected nuclei grow, and cellular chromatin becomes marginalized, to accommodate the growth of the replication compartments (36, 51).

Nuclear DNA is typically complexed in chromatin. The basic unit of chromatin is the nucleosome, 146 bp of DNA wrapped around a core histone octamer of two molecules each of H2A, H2B, H3, and H4. Linker histone H1 binds to DNA at the sites where it enters and exits the core nucleosome, promoting the formation of higher-order chromatin structures. Latent HSV-1 genomes are regularly chromatinized and, with the exception of LAT, transcriptionally silent (1, 8, 59). Digestion of latent HSV-1 genomes with micrococcal nuclease consequently produces a ladder of DNA fragments sized in multiples of 146 bp (8). Transcriptionally active lytic HSV-1 genomes, in contrast, are not regularly chromatinized, and their digestion with micrococcal nuclease mainly produces heterogeneously sized DNA fragments (25, 38, 39). They were therefore classically considered not to interact with histones. However, recent chromatin immunoprecipitation analyses have demonstrated that histone H3 binds to HSV-1 genomes (18, 19, 23, 40), as well as a relative depletion of H3, or enrichment of H3 bearing modifications of transcribed chromatin, at active HSV-1 promoters (18, 19, 23). It is now commonly accepted that HSV-1 genomes interact with histones during lytic infection too.

The expression of HSV-1 genes is temporally regulated. The immediate-early (IE) genes are expressed first, followed by the early (E) and then the late (L) ones. The virion protein VP16, in complex with two cellular proteins (oct-1 and host cell factor) binds to TAATGARAT sequences in IE promoters and recruits cellular general transcription factors and RNA polymerase II. The IE proteins ICP0 and ICP4 then activate E gene transcription (10). However, the specific mechanisms of E gene transactivation by ICP0 or -4 have not yet been fully characterized. They do not activate transcription by binding to specific DNA sequences and, consequently, they activate transcription driven by non-HSV-1 promoters recombined into HSV-1 genomes (52, 53).

Consistent with histones binding to lytic HSV-1 genomes, all HSV-1 transcription transactivators disrupt chromatin. VP16 promotes the depletion of H3 from HSV-1 genomes and recruits histone-modifying and other chromatin-remodeling complexes characteristic of transcription activation (18, 34, 63, 67). High mobility group (HMG) proteins enhance the transactivation activity of ICP4 (42), and they also compete with H1 for chromatin binding sites (5, 6). ICP0 induces the degradation of centromere proteins such as CENP A, an H3 variant (11, 28, 29). ICP0 also disrupts histone-modifying complexes

* Corresponding author. Mailing address: 327 Heritage Medical Research Centre, Edmonton, Alberta T6G 2S2, Canada. Phone: (780) 492-6265. Fax: (780) 492-3383. E-mail: luis.schang@ualberta.ca.

▽ Published ahead of print on 25 June 2008.

associated with chromatin condensation or inactivation of transcription (13, 14, 30).

In the absence of functional VP16, ICP0, and ICP4, HSV-1 genomes are transcriptionally inactive or quiescent (16, 45). Quiescent HSV-1 genomes associate with histones, too, and the chromatin associated with these genomes contains modifications and proteins characteristic of silenced heterochromatin (7, 12, 46). In the absence of only two transcriptional activators, VP16 and ICP0 (as in the mutant strain KM110), HSV-1 also establishes quiescent infections in some cell lines, such as Vero cells, but replicates (with delayed kinetics) in others, such as U2OS cells (37). Even in the absence of only one transactivator, such as in the ICP0 mutant strain n212, HSV-1 replicates with delayed kinetics in some cell types (Vero) (3).

The associations of histones with HSV-1 genomes during lytic infection are not yet fully characterized. Nonetheless, HSV-1 genomes are associated in some type of chromatin or chromatin-like structure, and histones H1 and H2B localize to early replication compartments (36, 50, 51). HSV-1 genomes are not associated with histones within virions, however, and are deposited in nuclear domains adjacent to ND10s, which are devoid of cellular chromatin (2, 20, 33, 40). The viral replication compartments are again depleted of histones (H1, H2B, H4, and serine 10-phosphorylated H3) later during infection (36, 50, 51, 58). Presently, the processes whereby histones come to interact with HSV-1 genomes early after infection, to be displaced later on, remain unknown. However, histones normally dissociate or are displaced from chromatin, diffuse, and rebind at different sites. Such mobilization is regulated by, for example, competition for the chromatin binding sites or posttranslational modifications. We therefore evaluated whether HSV-1 infection deregulates histone mobilization.

Here we show that linker histones are mobilized during HSV-1 infection, resulting in increases in the pools of "free" H1. Nuclear native HSV-1 genomes, but not HSV-1 proteins, were required for basal H1.2 mobilization, whereas IE or E HSV-1 proteins were required to further enhance H1.2 mobilization and increase its free pool. Such H1.2 mobilizations are consistent with IE or E HSV-1 protein expression inducing or requiring them. In either case, mobilization of linker histones during HSV-1 infection is a novel consequence of cell-virus interactions that is consistent with the dynamic interactions between histones and HSV-1 genomes. Histone mobilization could also play a role in the regulation of viral gene expression.

MATERIALS AND METHODS

Cells, viruses, and drugs. African Green monkey (Vero) cells were maintained in Dulbecco's modified minimum Eagle's medium (DMEM), supplemented with 5% fetal bovine serum (FBS), 50 U/ml penicillin, and 50 μg/ml streptomycin, at 37°C in 5% CO_2. Osteosarcoma (U2OS) cells, a generous gift from J. Smiley (University of Alberta), were maintained in DMEM supplemented with 10% FBS, 50 U/ml penicillin, and 50 μg/ml streptomycin at 37°C in 5% CO_2. Phosphonoacetic acid (PAA; Sigma) was prepared in DMEM as a 100-mg/ml stock and stored at −20°C. PAA was added to the medium at a concentration of 400 μg/ml and maintained throughout the course of infection.

Plasmids. The green fluorescent protein (GFP)-H1 plasmids (GFP-$H1^0$, GFP-H1.1, GFP-H1.2, GFP-H1.3, GFP-H1.4, and GFP-H1.5) were described previously (62). Briefly, DNA sequences encoding the H1 variants were PCR amplified from human neuroblastoma cell (SK-N-SH) genomic DNA. The 5′ primer contained a flanking BglII restriction site and the 3′ primer a flanking BamH1 site for directional in-frame cloning into pEGFP-C1 (Clontech).

Virus stock preparation. Wild-type HSV-1, strain KOS (passage 10), and mutant strains n212 (P. Schaffer, Harvard Medical School) and KM110 (J. Smiley, University of Alberta) have been described previously (4, 37, 54). For preparation of KOS stocks, Vero cells were seeded at 50 to 60% confluence in T-150 flasks and infected with 0.05 to 0.1 PFU per cell in 3 to 4 ml of DMEM. After 1 h of adsorption at 33°C, rocking and rotating every 10 min, inocula were removed and cells were washed twice with 4°C phosphate-buffered saline (PBS; 150 mM NaCl, 1 mM KH_2PO_4, 3 mM Na_2HPO_4, pH 7.4). Thirteen to 15 ml of 33°C DMEM supplemented with 10% FBS was added, and the cells were further incubated at 33°C. Cells were harvested at 95% or greater cytopathic effect and pelleted at 3,200 × *g* for 20 min at 4°C. Extracellular virions were pelleted from the resulting supernatant by centrifugation at 10,000 × *g* for 2 h at 4°C. Intracellular virions were isolated from the cell pellet through three cycles of freeze-thawing followed by sonication. Cellular debris were pelleted by centrifugation at 3,200 × *g* for 20 min at 4°C. Intra- and extracellular virions were combined for the viral stock. KOS titers were determined by standard plaque assay on Vero cells. Preparation of n212 stocks was as for KOS, except that U2OS cells were used. n212 titers were determined by standard plaque assay on U2OS cells. Parallel titrations on Vero cells ensured a minimum 100-fold reduction in titer (69).

For preparation of KM110 stocks, U2OS cells were seeded to 50% confluence in T-150 flasks and infected with 0.05 PFU per cell in 3 to 4 ml of DMEM supplemented with 5 mM *N,N′*-hexamethylene-bisacetamide (HMBA; Sigma). After incubation at 33°C, rocking and rotating every 10 min, 10 ml of 33°C DMEM supplemented with 10% FBS and 5 mM HMBA was added. Cells were harvested at 95% or greater cytopathic effect and virions were isolated as for KOS stock preparation. KM110 titers were determined by standard plaque assay on U2OS cells in the presence of 5 mM HMBA. Parallel titrations on Vero cells ensured a minimum 1,000-fold reduction in titer (37). All viral stocks were stored in DMEM at −80°C.

UV inactivation of HSV-1. A KOS stock was centrifuged at 10,000 × *g* for 1.5 h, and the pellet was resuspended in 4°C PBS. An aliquot was reserved and titrated on Vero cells. Additional aliquots were UV inactivated in a Stratalinker 1800 (Stratagene) and titrated. Stocks with titer reductions of 5 to 6 orders of magnitude which still fully transactivated a VP16-inducible promoter (M. R. St. Vincent and L. M. Schang, unpublished observations) were used. Inactivated stocks were stored in PBS at −80°C.

Transfection. Vero (2×10^5 to 3×10^5) or U2OS (1.4×10^5 to 2×10^5) cells were seeded in six-well plates and incubated at 37°C overnight. Plasmid DNA was transfected using Lipofectamine 2000 (Invitrogen). For each well to be transfected, Lipofectamine 2000 (4 μl or 2 μl for Vero or U2OS cells, respectively) was added to an Eppendorf tube containing 100 μl DMEM, and plasmid DNA (typically 3 or 1.5 μg for Vero or U2OS cells, respectively) was added to another. The plasmid-DNA mix was added to the Lipofectamine mix after a 10-min incubation at room temperature. Following an additional 30 (U2OS) or 60 (Vero) min of incubation at room temperature, the volume in each Eppendorf was brought to 1 ml with DMEM. Medium was then removed from the cells, they were overlaid with the transfection mix and incubated at 37°C for 4 (U2OS) or 6 (Vero) h, and then 1 ml of 37°C DMEM supplemented with 10% FBS was added to each well. Cells were further incubated at 37°C for at least 12 h before any other procedure.

HSV-1 infection. Transfected cells were seeded onto 18- by 18-mm coverslips (thickness 1; Fisher Scientific) in six-well plates for fluorescence recovery after photobleaching (FRAP) (typically, 3.4×10^5 to 4.0×10^5 Vero and 1.6×10^5 to 2.0×10^5 U2OS cells), or 12-mm-diameter circle coverslips (thickness 1D; Fisher Scientific) in 24-well plates for immunofluorescence (typically, 1×10^5 Vero and 0.8×10^5 U2OS cells). Seeded cells were incubated at 37°C for at least 4 h before infection. Inoculum was prepared by diluting purified HSV-1 stocks in 4°C DMEM. For mock infections, 4°C DMEM was used. A minimum volume of inoculum (400 or 150 μl for 6- and 12-well plates, respectively) was used to overlay the cells before incubation at 37°C for 1 h, rocking and rotating every 10 min. Inocula were removed, and cells were washed twice with 4°C PBS and overlaid with 37°C DMEM supplemented with 5% or 10% FBS for Vero or U2OS cells, respectively.

FRAP. Histone mobilization was evaluated from 4 to 5 or 7 to 8 h postinfection (hpi). Prepared slides were used for less than 1 h of data collection, to ensure cell viability. Slides were prepared by placing a 1/2-in. round adhesive template in the center. A thin layer of vacuum grease was applied around the template, which was then removed and replaced with medium from the well containing the coverslip. The coverslip was mounted cell side down, forming a sealed chamber. Isopropanol was applied to the end of the slide and run over the coverslip. The slide was then promptly placed on a 37°C stage on a Zeiss NLO 510 multiphoton microscope. Cells were viewed on a 37°C 40× F-Fluor oil immersion objective

lens (numerical aperture, 1.3; working distance, 0.12 mm). FRAP was performed using a 25-mW argon laser (488 nm) with a band-pass filter of 505 to 530 nm and a pinhole of 1,000 (~15 Airy units). A 1.5-μm-wide region passing across the cell nucleus was photobleached, typically with 30 iterations at 100% intensity. Fixed cells expressing GFP-H1 were used to ensure complete photobleaching. Whole-cell imaging was performed at 0.5 to 1% intensity. Sixty fluorescent and differential interference contrast images (512 by 512; 12 bit) were collected for each experiment at timed intervals before and after bleaching. Images were analyzed with Zeiss LSM software, and contrast and brightness were adjusted for figure preparation with Adobe Photoshop.

Immunofluorescence. Infected cells were washed with 4°C PBS and fixed with 5% formaldehyde at room temperature for 10 or 15 min, followed by four washes with 4°C PBS. All subsequent washes and incubations were performed at room temperature unless otherwise indicated. The cells were permeabilized for 6 min with CSK buffer [0.5% Triton X-100, 10 mM piperazine-*N*,*N*′-bis(2-ethanesulfonic acid) (pH 6.8), 50 mM NaCl, 300 mM sucrose, 3 mM $MgCl_2$] or −20°C 100% methanol for 1 min. After PBS washes, cells were incubated in blocking buffer (4% normal goat serum, 2% bovine serum albumin in PBS) for 1 h with slow rocking. Mouse monoclonal anti-ICP4 (catalog no. 1101-897; Goodwin Institute for Cancer Research Inc., Plantation, FL) diluted 1:10,000 in blocking buffer was added, and the cells were further incubated for 2 h with slow rocking before washing twice with 0.05% Tween in PBS, or thrice with PBS, for 10 min each. AlexaFluor 594-labeled goat anti-mouse antibody (Molecular Probes) diluted 1:1,000 in blocking buffer was added for 1 h with slow rocking, followed by two washes of 10 min each with 0.05% Tween in PBS or three washes of 10 min each with PBS. Nuclei were counterstained with 1 μg/ml Hoechst 33258 for 5 min and then washed twice with PBS. Coverslips were rinsed in distilled deionized H_2O, mounted onto slides with Vectashield mounting medium (Vector), and sealed with clear nail enamel. The cells were viewed on a Leica DM IRB microscope. A minimum of 90 transfected and 300 nontransfected cells from at least two experiments were counted for each H1 variant at 4 and 7 hpi, except for $H1^0$, H1.4, and H1.5 at 7 hpi, for which a minimum of 50 transfected and 90 nontransfected cells were counted from one experiment. For infections with HSV-1 mutant strains, a minimum of 170 or 214 transfected and 488 or 414 nontransfected Vero or U2OS cells, respectively, were counted from at least two experiments, except for strain n212 at 4 hpi in Vero cells, for which 60 transfected and 245 nontransfected cells were counted from one experiment, and at 7 hpi in U2OS cells, for which 128 transfected and 168 nontransfected cells were counted from one experiment. For Vero cells infected with UV-inactivated KOS, 25 and 40 transfected cells were counted at 4 and 7 hpi, respectively, and 150 nontransfected cells were counted at 4 and 7 hpi from one experiment. For U2OS cells infected with UV-inactivated KOS, a minimum of 80 transfected and nontransfected cells were counted at 4 and 7 hpi from one experiment.

Confocal images were collected with Zeiss laser scanning confocal (LSM 510) or multiphoton (NLO 510) microscopes, on a 40× F-Fluor oil immersion objective (numerical aperture, 1.3; working diameter, 0.12 mm) using 25-mW argon (488 nm) and 1-mW HeNe (543 nm) lasers with band-pass filters of 500 to 550 and 548 to 623 or a long-pass filter of 560 nm, respectively. Imaging was performed at 5% or 100% of the argon or HeNe laser intensity, respectively, with pinholes set at ~1.5 Airy units for each. Fluorescent images (512 by 512; 12 bit) were analyzed with Zeiss LSM software; image contrast and brightness were adjusted for figure preparation using Adobe Photoshop.

RESULTS

Somatic linker histone variants are differentially mobilized in HSV-1-infected cells. Our first objective was to test whether histones are mobilized in HSV-1-infected cells. To this end, we used FRAP in cells expressing GFP-histone H1 fusion proteins. GFP-H1 fusion proteins behave as endogenous H1, and moderate levels of expression do not adversely affect the expressing cells (27, 35). However, the effects of GFP-H1 fusion protein expression on HSV-1 replication were unknown. We therefore first analyzed ICP4 expression in cells expressing different GFP-H1 fusion variants (Table 1 shows the H1 variant nomenclature). Progression of HSV-1 infection, as evaluated by immunofluorescence against ICP4, was not adversely affected by the expression of moderate levels of any GFP-H1 variant (Fig. 1 and 2). At 4 or 7 hpi, cells expressing any of the GFP-H1 variants had similar expression of ICP4 and also similar ICP4 accumulation into replication compartments as cells not expressing any GFP-H1 (Fig. 1, examples of ICP4 as nuclear diffuse or in replication compartments in cells expressing GFP-H1; Fig. 2, quantitation). The nuclear localization of GFP-H1 was maintained even at late times postinfection (Fig. 1). These experiments also confirmed previously published results (36, 50, 51, 58) showing histones colocalizing with early replication compartments but mostly displaced from them at later times (Fig. 1A, right-most panels).

TABLE 1. Nomenclatures of the H1 variants used in this work

H1 variant			Accession no.
Doenecke[a]	Parseghian[b]	Seyedin[c]	
$H1^0$			NP_005309
H1.1	H1a	H1a	NP_005316
H1.2	$H1^s$-1	H1c	NP_005310
H1.3	$H1^s$-2	H1d	NP_005311
H1.4	$H1^s$-4	H1e	NP_005312
H1.5	$H1^s$-3	H1b	NP_005313

[a] From Doenecke et al. (9); this is the nomenclature used in our work.
[b] From Parseghian et al. (43).
[c] From Seyedin et al. (48).

As a first test for histone mobilization, we analyzed the FRAP recovery kinetics of different GFP-H1 variants in Vero cells infected for 7 h with HSV-1 KOS. Mobilization was evaluated by the time to recover 50% of the original fluorescence (T_{50}) in the photobleached area. Mobilization and T_{50} are inversely related, such that a higher degree of mobilization results in a shorter T_{50}. All H1 variants except for H1.4 were significantly mobilized in cells infected with 30 PFU/cell of KOS ($P < 0.05$) (Table 2; Fig. 3), although the individual variants were differentially mobilized. H1.2 was mobilized the most; its T_{50} was reduced to less than half (42.3%) of that in mock-infected cells (T_{50}, 6.9 ± 0.5 and 14.8 ± 0.4 s, respectively) (means ± standard errors of the means) (Table 2; Fig. 3). The HSV-1- and mock-infected cells shown in Fig. 3C, for example, were equally photobleached with the same laser intensity and duration. However, H1.2 was mobilized to such an extent that the fluorescence in the photobleached region of the infected cell had already recovered at 4 s to a greater degree than in the mock-infected one. H1.1, H1.5, $H1^0$, and H1.3 were also mobilized, but to lesser degrees (T_{50} reduced to 57%, 59%, 63%, and 64% of those in mock-infected cells) (Table 2). H1.4 was apparently mobilized as well, but the mobilization was not statistically significant ($P = 0.08$; T_{50} of 66% of that in mock-infected cells) (Table 2; Fig. 3). Consistently, the fluorescence in the photobleached region of the HSV-1-infected cell expressing GFP-H1.4 had recovered at 4 s only to a similar degree as the mock-infected one (Fig. 3D).

The differential average mobilization of the H1 variants could have been due to differential mobilization of each variant in all infected cells, or to similar mobilization of each variant in different sized subpopulations of infected cells. Therefore, we evaluated the percentage of cells with the highest H1 mobilization, defined as those in which the T_{50} was >1 standard deviation (SD) below the average T_{50} in mock-infected cells. A similar percentage of infected cells had mobilized H1.1 or H1.5 to this extent (75% and 71%, respectively), and H1.1 and H1.5

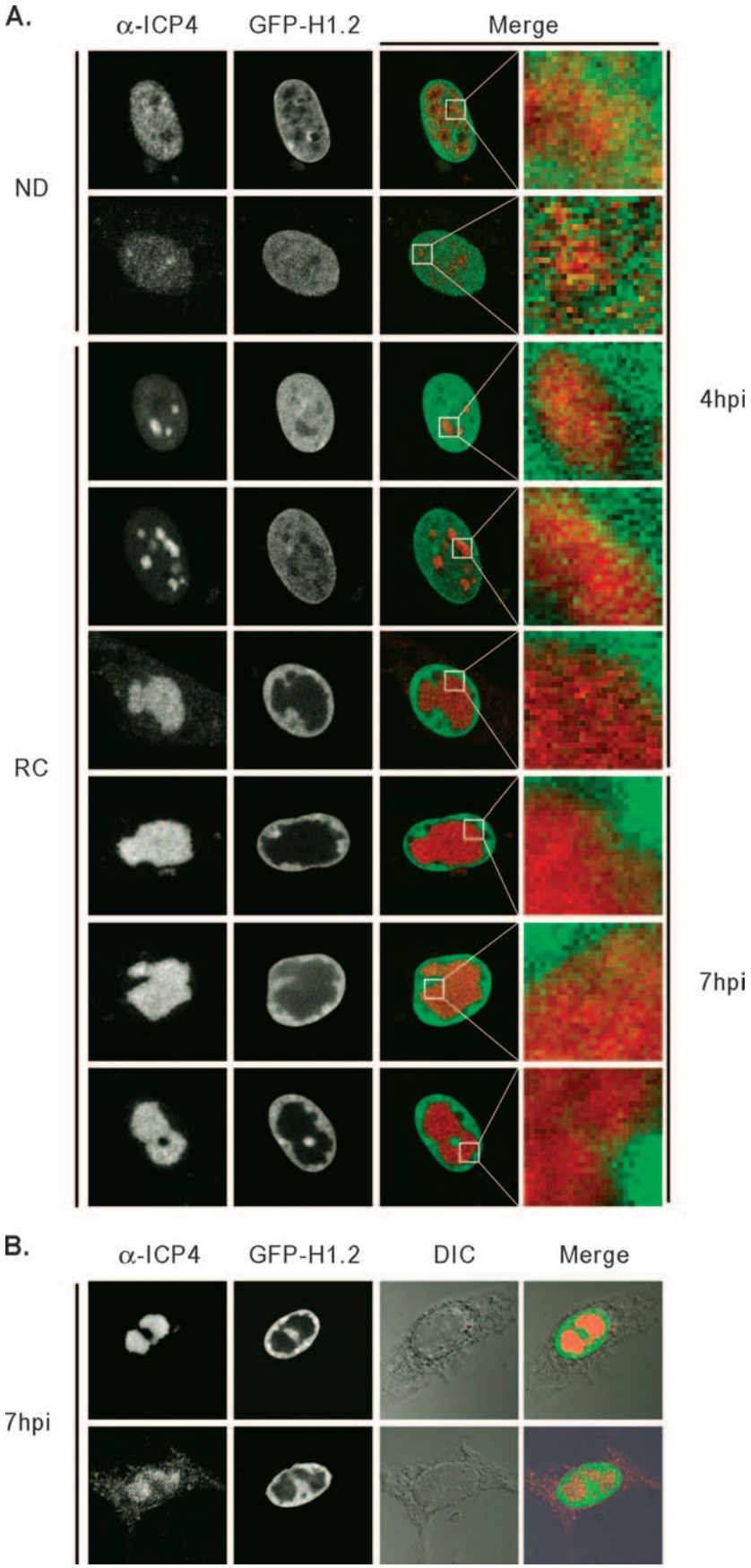
A.
α-ICP4
GFP-H1.2
Merge
ND
4hpi
RC
7hpi
B.
α-ICP4
GFP-H1.2
DIC
Merge
7hpi

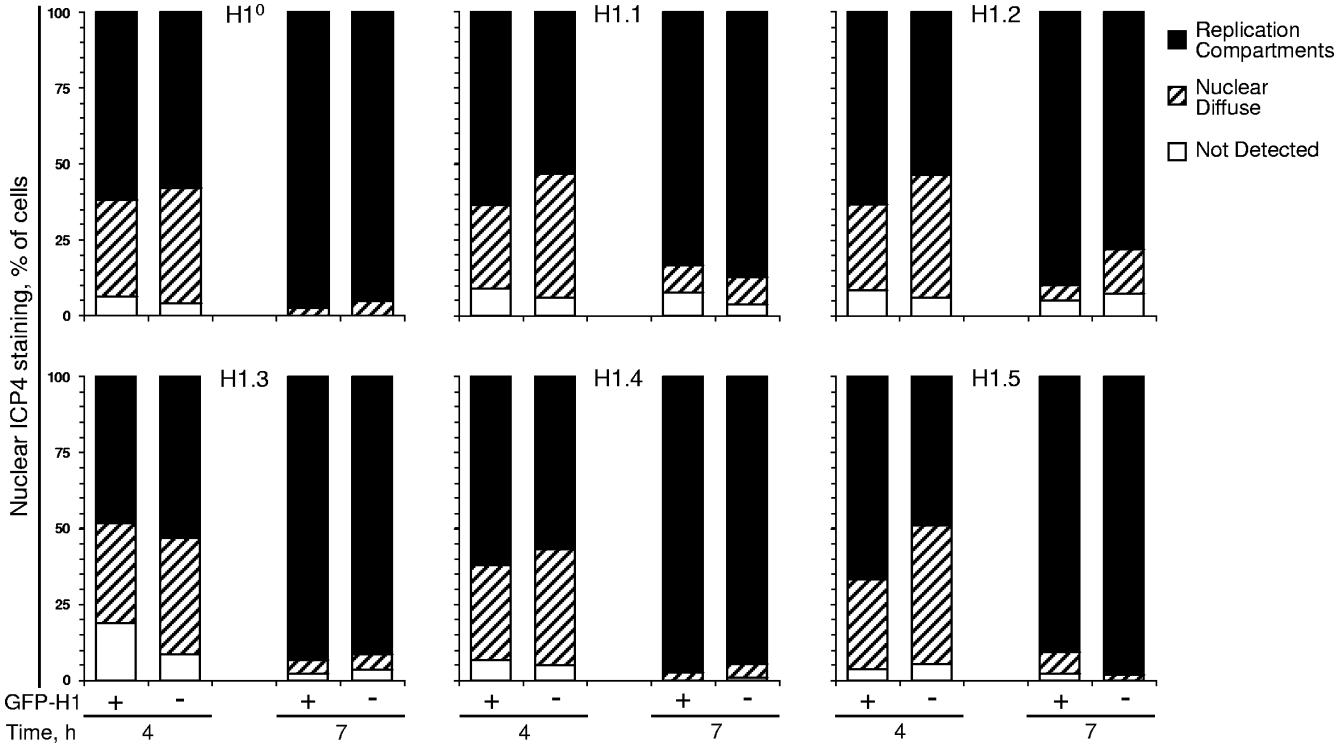

FIG. 2. ICP4 expression and accumulation into replication compartments in Vero cells expressing or not expressing GFP-H1 somatic variants. The bar graphs show the percentage of HSV-1-infected cells transfected with each GFP-H1 somatic variant and expressing ICP4 as nuclear diffuse or accumulated into replication compartments. Vero cells were transfected with plasmids expressing GFP fused to each H1 somatic variant ($H1^0$, H1.1, H1.2, H1.3, H1.4, and H1.5), infected with 30 PFU/cell HSV-1 strain KOS, fixed at 4.5 (4) or 7.5 (7) hpi, and stained for ICP4. Nuclear expression of ICP4 and accumulation into replication compartments (Fig. 1) in cells in which GFP-H1 was expressed (+) or not (−) was evaluated by fluorescence microscopy.

were also mobilized on average to a similar degree (57% and 59% of mock, respectively) (Table 2). However, more cells had mobilized H1.5 than $H1^0$ to this extent (71% and 52%, respectively), although these variants were also mobilized on average to a similar degree (59% and 63% of mock, respectively) (Table 2). The differential mobilization of each H1 variant is therefore a combination of the degree of mobilization in each cell together with the size of the population of cells that mobilize H1 to a certain degree.

H1 may be mobilized by cellular or viral factors. To identify such putative factors, we focused on H1.2, a variant that is biologically relevant for HSV-1. H1.2 is expressed in all cells that HSV-1 infects, and its expression is cell cycle independent (44). Moreover, H1.2 was mobilized the most, and the vast majority of infected cells (92%) had mobilized H1.2 to more than 1 standard deviation below the average T_{50} in mock-infected cells.

H1.2 is already mobilized at early times postinfection, but it is further mobilized at later times. We had initially evaluated mobilization at 7 hpi, when all HSV-1 proteins are expressed and HSV-1 genomes are replicated. HSV-1 protein expression, DNA replication, or cellular responses to them may therefore contribute to the mobilization of linker histones. The number of different HSV-1 proteins expressed, their levels, and the number of viral genomes increases as infection proceeds. We therefore also evaluated H1.2 mobility at early times postinfection. H1.2 was already significantly mobilized at 4 hpi ($P < 0.01$), when IE and E proteins are expressed to high levels. Its T_{50} was decreased to 72% or 62% in cells infected with 10 or 30 PFU/cell, respectively (T_{50}, 9.3 ± 0.7 or 7.3 ± 0.6 s, respectively) (Table 3; Fig. 4A). H1.2 was further mobilized at 7 hpi, when IE, E, and L proteins are expressed and genomes are replicated. Its T_{50} was decreased to 61% or 42% in cells infected with 10 or 30 PFU/cell, respectively (T_{50}, 9.4 ± 1.0 or 6.9 ± 0.5 s, respectively;

FIG. 1. Expression of ICP4 as nuclear diffuse or accumulated into replication compartments in Vero cells expressing GFP-H1.2. Digital fluorescent micrographs show Vero cells expressing GFP-H1.2 and stained with anti-ICP4 (α-ICP4) antibodies. Cells were transfected with plasmids expressing GFP fused to H1.2 and infected with 30 PFU/cell of HSV-1 strain KOS. Cells were fixed at 4.5 (4) or 7.5 (7) hpi as indicated and stained for ICP4. Single (anti-ICP4 [α-ICP4], GFP-H1.2, and differential interference contrast [DIC]) and merged images are shown. (A) Cells with ICP4 expressed as nuclear diffuse (ND) or replication compartments (RC). Right-most panels, 16× digital enlargement of the regions indicated by the boxes on the left-most merge images, highlighting the colocalization of H1.2 and ICP4 signals (pixels in different shades of yellow and orange). (B) Cells showing strictly nuclear localization of GFP-H1.2 regardless of whether the ICP4 signal is nuclear (top) or nuclear and cytoplasmic (bottom). The GFP-H1.2 images were overexposed to highlight the lack of cytoplasmic signal.

TABLE 2. Mobility of somatic H1 variants in mock- and HSV-1-infected cells

H1 variant	T_{50} (s) (avg ± SEM)		HSV/mock ratio (%) (avg ± SEM)	% Cells with high H1 mobilization[a]
	Mock	HSV		
$H1^0$	23.6 ± 2.0	15.2 ± 1.8	63.3 ± 6.7	52
H1.1	27.3 ± 1.8	13.4 ± 1.3	57.0 ± 7.2	75
H1.2	14.8 ± 0.4	6.9 ± 0.5	42.3 ± 3.4	92
H1.3	23.1 ± 2.8	13.7 ± 1.8	63.8 ± 10.1	69
H1.4	49.5 ± 8.1	32.5 ± 5.3	66.4 ± 7.0	60
H1.5	43.1 ± 5.4	26.4 ± 5.2	59.3 ± 10.8	71

[a] Percentage of cells in which the T_{50} was >1 SD lower than the average T_{50} in mock-infected cells.

$P < 0.01$) (Table 3; Fig. 4A). These results suggest that expression of specific HSV-1 proteins or HSV-1 DNA replication augment H1.2 mobilization.

Concomitant with the increase in H1.2 mobilization, the population of cells with the highest H1.2 mobilization had also increased from 4 to 7 hpi (from 36% to 63%, or 61% to 92% for cells infected with 10 or 30 PFU/cell, respectively) (Table 3; Fig. 4B). The size of this population was also dependent on the multiplicity of infection. At both early and late times, a larger population infected with 30 than with 10 PFU/cell had such high H1.2 mobilization.

The mobilization of H1.2 may result from changes in its low- or high-affinity binding to chromatin, or in the residence time (the time that it is bound to chromatin). We next evaluated the time required to recover 90% of the original fluorescence in the photobleached region (T_{90}). Whereas T_{50} is influenced the most by low-affinity binding, T_{90} is influenced the most by high-affinity binding. As with T_{50}, H1.2 T_{90} was decreased in HSV-1-infected cells at early and late times postinfection (30 PFU/cell 4 and 7 hpi and 10 PFU/cell at 7 hpi [$P < 0.01$]; 10 PFU/cell at 4 hpi [not significant]) (Table 3; Fig. 4A). Moreover, the relative decreases in H1.2 T_{50} and T_{90} were not significantly different from each other ($P > 0.05$). Thus, the mobilization of H1.2 resulted from changes in both low- and high-affinity chromatin binding.

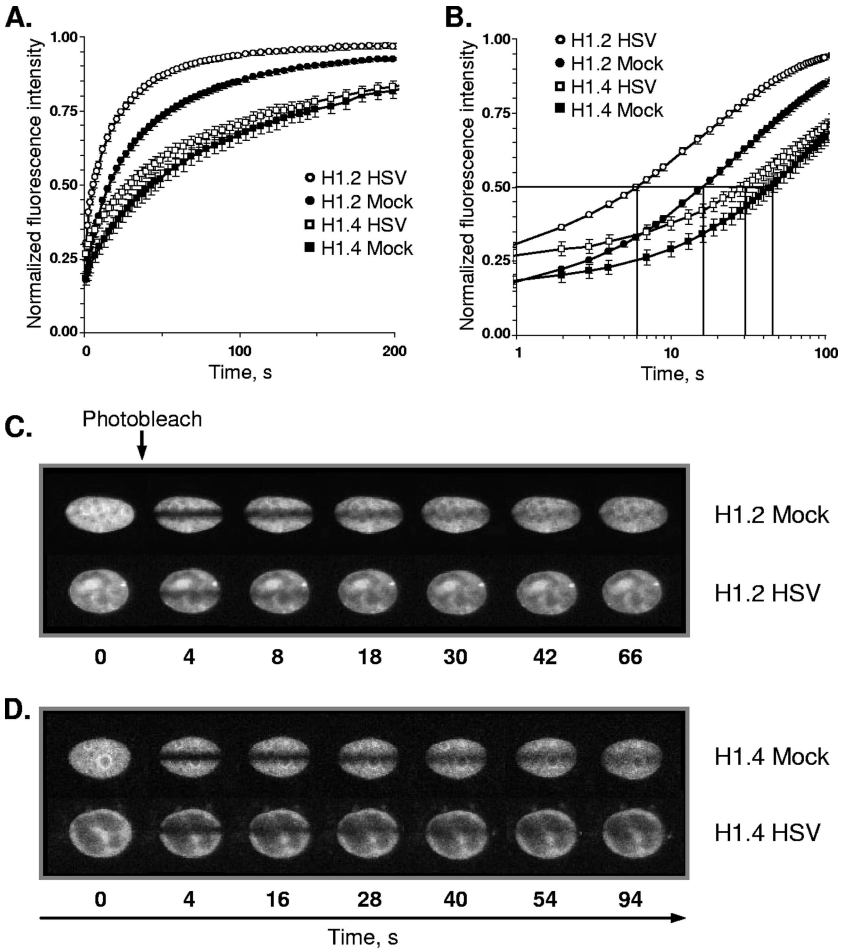

FIG. 3. Somatic linker histone variants are differentially mobilized in HSV-1-infected cells. (A) Line graphs representing the normalized fluorescence intensity of the photobleached nuclear region versus time. Vero cells were transfected with plasmids expressing GFP fused to H1.2 or H1.4. Transfected cells were mock infected or infected with 30 PFU/cell of HSV-1 strain KOS. Nuclear mobility of each GFP-H1 variant was examined from 7 to 8 hpi by FRAP. Error bars indicate the standard errors of the means ($n \geq 15$); time is plotted on a linear scale. (B) The same data as in panel A, presented on a semilogarithmic scale. Lines indicate the times when 50% of the original relative fluorescence was recovered (T_{50}). (C and D) Composite images of Vero cells expressing GFP-H1.2 (C) or GFP-H1.4 (D) infected as described for panel A. Images were collected prior to (time zero) or at the indicated times after photobleaching.

TABLE 3. Mobilization of H1.2 in Vero cells infected with wild-type or mutant HSV-1 strains

Time (hpi)	Virus strain	PFU/cell	T_{50} (avg ± SEM)		% Cells with high H1 mobilization, T_{50}[a]	T_{90} (avg ± SEM)		% Cells with high H1 mobilization, T_{90}[b]
			Absolute (s)	Relative (%)		Absolute (s)	Relative (%)	
4			13.2 ± 0.4	100	13	110.1 ± 2.8	100	11
	KOS	10	9.3 ± 0.7	72 ± 6	36	87.8 ± 7.0	80 ± 8	31
		30	7.3 ± 0.6	62 ± 5	61	69.1 ± 6.0	63 ± 6	42
	n212	10	9.9 ± 0.6	74 ± 5	52	79.0 ± 5.5	72 ± 6	38
		30	8.7 ± 0.6	72 ± 5	44	83.7 ± 5.6	76 ± 6	31
		60	7.0 ± 0.8	54 ± 6	78	60.9 ± 6.8	55 ± 7	78
	KM110	10, 30, or 60	11.5 ± 0.4	81 ± 3	32	93.8 ± 3.3	85 ± 3	29
	UV	10, 30, or 60	12.9 ± 0.5	98 ± 4	19	94.6 ± 3.9	86 ± 4	21
7			14.8 ± 0.4	100	17	112.3 ± 2.9	100	16
	KOS	10	9.4 ± 1.0	61 ± 4	63	76.8 ± 5.9	68 ± 4	63
		30	6.9 ± 0.5	42 ± 3	92	65.0 ± 4.5	58 ± 5	74
	n212	10	9.3 ± 0.9	64 ± 5	58	89.3 ± 8.7	80 ± 8	43
		30	7.1 ± 0.6	54 ± 4	83	76.6 ± 3.4	68 ± 3	71
		60	5.0 ± 0.7	41 ± 5	82	66.1 ± 9.6	59 ± 10	71
	KM110	10, 30, or 60	11.7 ± 0.4	78 ± 3	40	97.7 ± 3.7	87 ± 3	29
	UV	10, 30, or 60	13.2 ± 0.5	95 ± 4	27	102.7 ± 5.0	91 ± 5	33

[a] Percentage of cells in which the T_{50} was >1 SD lower than the average T_{50} in mock-infected cells.
[b] Percentage of cells in which the T_{90} was >1 SD lower than the average T_{90} in mock-infected cells.

To address whether the mobilization of H1.2 affected the residence time, we evaluated the level of H1.2 in the so-called free pool (i.e., not bound to chromatin). The surrogate measure for the free pool is the level of recovery of fluorescence at the first time point after photobleaching. Fixed cells show no recovery (i.e., complete bleaching) at this (or any other) time point. The recovery of fluorescence in live cells at the first time point therefore reflects only the very rapidly diffusing histone molecules, which are considered unbound to chromatin (i.e., free). The pool of free H1.2 was significantly increased to 119% ± 5% in Vero cells infected with 10 or 30 PFU/cell of KOS at 4 hpi and remained increased at 7 hpi (to 141% ± 7% or 174% ± 6%, respectively; $P < 0.01$) (Table 4; Fig. 5A, KOS 30). The relative binding to and dissociation or displacement from chromatin are therefore differentially altered in infected cells, such that a larger population of H1.2 is not bound to chromatin at any given time.

To evaluate the percentage of infected cells with an increased pool of free H1.2, we considered the cells with the largest pools of free H1.2, defined as those in which such a pool was greater than 1 standard deviation above the average level of free H1.2 in mock-infected cells. More than 50% of cells had pools of free H1.2 increased to this extent at any time (Table 4). Therefore, the level of free H1.2 is increased throughout the population of infected cells.

Early and late H1.2 mobilizations therefore occur through changes to both low- and high-affinity binding to chromatin. Furthermore, the chromatin residence time of H1.2 is altered such that there is a net increase in the pool of H1.2 not bound to chromatin at any given time.

H1.2 mobilization does not require VP16 or ICP0, whereas free H1.2 increases in their absence only if HSV-1 proteins are expressed. To test whether specific HSV-1 proteins contributed to mobilization, we used the HSV-1 strain KM110, which is mutated in ICP0 (stop codon at codon 212) and VP16 (stop codon at codon 422) (37). KM110 fails to activate IE gene expression and, as a result, cannot replicate in Vero cells.

ICP4 was undetectable in more than 90% or 85% of cells infected with 30 PFU/cell of KM110 at 4 or 7 hpi, respectively (Table 5; Fig. 6, KM110 Vero), regardless of whether they expressed GFP-H1.2 or not. In the cells in which it was detected, ICP4 was mainly nuclear diffuse. Less than 2% of cells had ICP4 accumulation into (mostly small) replication compartments (Table 5; Fig. 6, KM110 Vero). H1.2 was nonetheless mobilized at early and late times, independently of the multiplicity of infection (10, 30, or 60 PFU/cell; $P > 0.05$, pairwise comparisons, Tukey's honestly significantly different [HSD] test). We therefore analyzed all multiplicities together. H1.2 T_{50} was decreased to 80% of mock-infected cells at 4 or 7 hpi in cells infected with 10, 30, or 60 PFU/cell (T_{50}, 11.6 ± 0.3 s; $P < 0.01$) (Table 3; Fig. 7, KM110 Vero). Like in KOS-infected cells, H1.2 mobilization in KM110-infected cells was a result of changes in both low- and high-affinity binding. H1.2 T_{50} and T_{90} were decreased to similar extents ($P > 0.05$) (Table 3). In contrast to cells infected with KOS, however, neither the average H1.2 mobilization nor the size of the population with the highest mobilization of H1.2 was further increased at later times.

Although H1.2 was mobilized, the average levels of free H1.2 were not increased at either early or late times postinfection (at 10, 30, or 60 PFU/cell; $P > 0.05$) (Table 4; Fig. 5A, KM110). The relative rates of H1.2 binding and dissociation or displacement were therefore equally altered such that there was no net increase in the pools of free H1.2.

Taken together, these results show that the basal mobilization of H1.2 was independent of VP16 and ICP0 and occurred under conditions in which there was little to no HSV-1 protein expression. In contrast, VP16, ICP0, HSV-1 transcription, specific HSV-1 proteins, or genome replication is required to enhance the basal mobilization of H1.2 and to increase its free pool. Alternatively, the increase in the pool of free H1.2 may be required for HSV-1 gene expression.

Both VP16 and ICP0 disrupt chromatin (11, 18, 28–30, 34, 63). To test whether their biochemical activities were directly involved in H1.2 mobilization, we analyzed KM110 infections

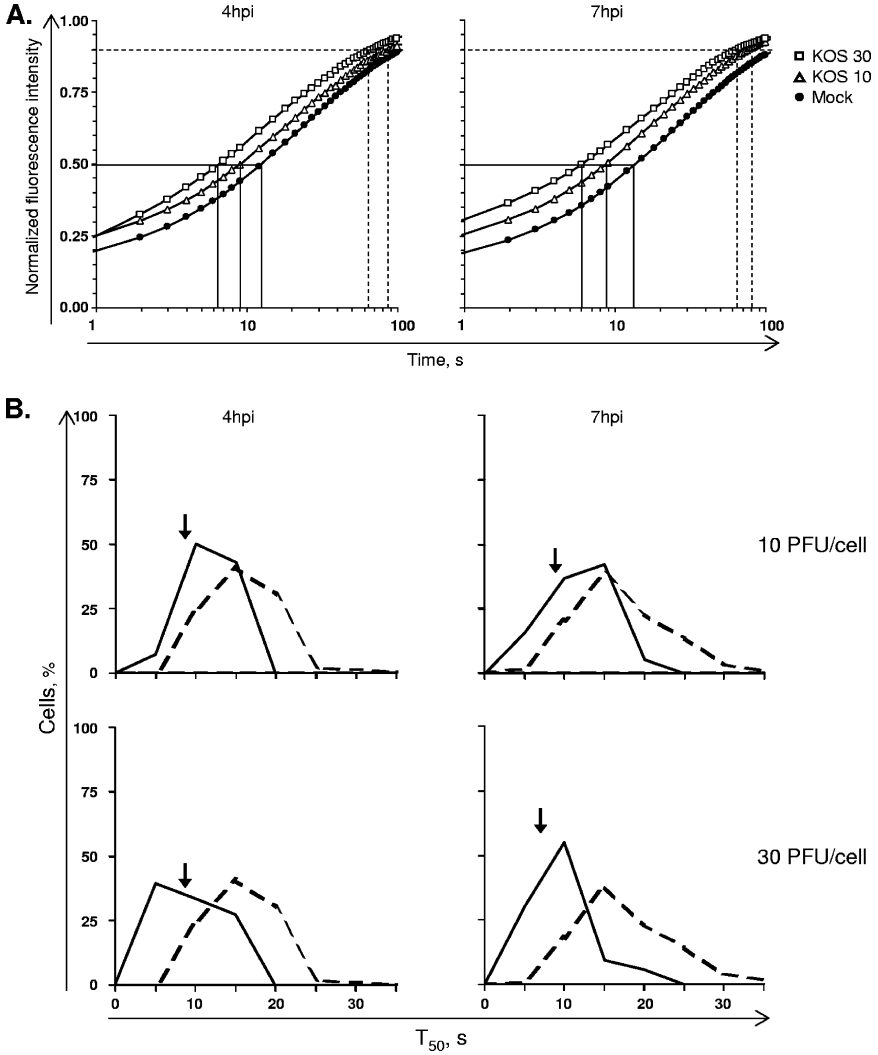

FIG. 4. H1.2 mobilization increases with multiplicity of infection and time after infection. (A) Line graphs representing the normalized fluorescence intensity of the photobleached nuclear region over time. Vero cells were transfected with plasmids expressing GFP-H1.2 and mock infected or infected with 10 or 30 PFU/cell of HSV-1 strain KOS. Nuclear mobility of GFP-H1.2 was examined from 4 to 5 hpi (4 hpi) or 7 to 8 hpi (7 hpi) by FRAP. Solid or dashed lines are the times when 50 or 90% of the original relative fluorescence was recovered (T_{50} or T_{90}), respectively. Mock-infected cells had not recovered 90% of the original relative fluorescence when the measurements were stopped at 100 s. (B) Frequency distribution plots of the T_{50} per individual cell as evaluated by FRAP. Dashed or solid lines, mock-infected or HSV-1 strain KOS-infected cells, respectively; arrows, mean T_{50} of the infected cell population ($n \geq 14$).

of U2OS cells. U2OS cells complement the replication defects of HSV-1 mutants in ICP0 or VP16 (69). Consequently, all HSV-1 proteins are expressed and HSV-1 DNA is replicated during KM110 infection of U2OS cells (37). U2OS cells, however, do not complement the known biochemical activities of ICP0 or VP16. At 4 hpi, 47% of U2OS cells infected with 30 PFU/cell of KM110 had nuclear diffuse ICP4, whereas 27% had accumulated it into replication compartments (Table 5; Fig. 6, KM110 U2OS). At 7 hpi, 26% of cells had nuclear diffuse ICP4, whereas in 63% it accumulated into replication compartments (Table 5; Fig. 6, KM110 U2OS). Cells expressing GFP-H1.2 or not had similar expression of ICP4 and similar ICP4 accumulation into replication compartments (Fig. 6, KM110 U2OS).

H1.2 was mobilized in U2OS cells in the absence of VP16 and ICP0. At early times postinfection, however, the degree of mobilization was dependent on the multiplicity of infection. H1.2 was significantly mobilized in U2OS cells infected with 30 PFU/cell (83% of mock-infected cells; $P < 0.01$) but not in those infected with 10 PFU/cell (96% of mock-infected cells; $P > 0.05$) (Table 6; Fig. 7, KM110 U2OS). At later times, H1.2 was further mobilized and the degree of mobilization was no longer dependent on the multiplicity of infection ($P > 0.05$, Tukey's HSD). H1.2 T_{50} was decreased to 54% of that in mock-infected cells in cells infected with 10 or 30 PFU/cell of KM110 (T_{50}, 5.9 $\pm$ 0.4 s) (Table 6; Fig. 7, KM110 U2OS). H1.2 was thus further mobilized at later times, alongside the increase in the number and levels of HSV-1 proteins expressed.

As in Vero cells, the mobilization of H1.2 at early and late times was a result of changes to both low- and high-affinity chromatin binding. The H1.2 T_{90} was decreased to a similar

TABLE 4. Levels of free H1.2 in cells infected with wild-type and mutant HSV-1 strains

Cell type	Virus strain	PFU/cell	4 hpi		7 hpi	
			Relative free H1.2 (avg ± SEM)	% Cells with large increase in free H1.2[a]	Relative free H1.2 (avg ± SEM)	% Cells with large increase in free H1.2[a]
Vero			1.00 ± 0.01	15	1.00 ± 0.02	15
	KOS	10	1.19 ± 0.05	64	1.41 ± 0.07	63
		30	1.19 ± 0.05	52	1.74 ± 0.06	92
	n212	10	1.15 ± 0.05	48	1.52 ± 0.09	71
		30	1.15 ± 0.04	35	1.45 ± 0.05	75
		60	1.36 ± 0.08	72	1.61 ± 0.09	88
	KM110	10, 30, or 60	1.08 ± 0.04	30	1.22 ± 0.03	49
	UV	10, 30, or 60	0.97 ± 0.03	13	1.03 ± 0.03	14
U2OS			1.00 ± 0.02	20	1.00 ± 0.02	19
	KOS	6	1.16 ± 0.06	53	1.78 ± 0.06	100
	n212	10 or 30	1.52 ± 0.03	95	1.84 ± 0.04	100
	KM110	10 or 30	1.13 ± 0.03	39	1.49 ± 0.04	89
	UV	30 or 60	1.00 ± 0.02	13	0.93 ± 0.02	5

[a] Percentage of cells in which the level of free H1.2 was >1 SD above the average level of free H1.2 in mock-infected cells.

extent as T_{50} at either multiplicity (T_{90} versus T_{50}, $P > 0.1$) (Table 6). Further, like KOS-infected Vero cells, free H1.2 was increased in KM110-infected U2OS cells in a multiplicity-independent manner ($P > 0.05$, Tukey's HSD). Free H1.2 was increased to 113% ± 3% ($P < 0.05$) at 4 hpi and to 149% ± 4% at 7 hpi ($P < 0.01$) (Table 4; Fig. 5B, KM110).

H1.2 was equally mobilized at late times in U2OS cells infected with KM110 or KOS, although the cells had to be infected with lower multiplicities of KOS because of the nuclear distortion at high multiplicities. Nonetheless, the H1.2 T_{50} was reduced to 66% or 40% in U2OS cells infected with 6 PFU/cell of KOS at 4 or 7 hpi, respectively (T_{50}, 8.0 ± 0.6 or 5.8 ± 0.4 s, respectively; $P < 0.01$) (Table 6; Fig. 7, KOS U2OS). Concomitantly, H1.2 T_{90} was also decreased at early and late times (Table 6), and free H1.2 was increased to 116% ± 6% at 4 hpi and to 178% ± 6% at 7 hpi ($P < 0.01$) (Table 4; Fig. 5B, KOS). The biochemical activities of VP16 or ICP0 were thus not required in U2OS cells to increase the pool of free H1.2 or to enhance its mobilization.

The degree of H1.2 mobilization and increase in free H1.2 are associated with HSV-1 protein expression or DNA replication. We next infected Vero cells with the ICP0 mutant strain n212 to test whether progression of infection was required to mobilize H1.2 above the basal level. n212 carries the same ICP0 mutation as KM110 but has wild-type VP16 (4). Unlike KM110, n212 genes are expressed and its DNA is replicated in Vero cells, although both are delayed at low multiplicities of infection (4).

As expected (4), 78% of cells infected with 30 PFU/cell of n212 had nuclear diffuse ICP4 at 4 hpi and only 11% had accumulated it into replication compartments, in comparison to 40% and 52% of cells infected with wild-type KOS, respectively (Table 5; Fig. 6). The population with ICP4 accumulated into replication compartments increased to 56% at 7 hpi, whereas that with nuclear diffuse ICP4 decreased to 37%, in comparison to 78% and 9% in cells infected with wild-type KOS, respectively (Table 5; Fig. 6). ICP4 accumulation into replication compartments was thus delayed relative to that in KOS-infected cells, but it was still independent of H1.2 (Fig. 6, n212 Vero).

H1.2 was also significantly mobilized in n212-infected Vero cells ($P < 0.01$). In contrast to KOS-infected ones, however, the mobilization was multiplicity dependent. At 4 hpi, the H1.2 T_{50} was decreased to 74%, 72%, and 54% in cells infected with 10, 30, or 60 PFU/cell of n212, respectively (T_{50}, 9.9 ± 0.6, 8.7 ± 0.6, and 7.0 ± 0.8 s, respectively) (Table 3; Fig. 7, n212 Vero) ($P < 0.05$ for 10 to 60 and 30 to 60 PFU/cell, Tukey's HSD). The H1.2 T_{50} was also decreased in a multiplicity-dependent manner at 7 hpi, to 64%, 54%, or 41% in cells infected with 10, 30, or 60 PFU/cell, respectively (T_{50}, 9.3 ± 0.9, 7.1 ± 0.6, or 5.0 ± 0.7 s, respectively) (Table 3; Fig. 7, n212 Vero) ($P < 0.01$, 10 to 60 PFU/cell, Tukey's HSD).

As in infections with KOS, H1.2 mobilization in n212-infected Vero cells was the result of changes to low- and high-affinity chromatin binding. Moreover, there was also a net increase in the pools of free H1.2. In contrast to KOS-infected cells, however, the increase in free H1.2 in n212-infected cells was also dependent on multiplicity ($P < 0.05$ for 10 to 60 and 30 to 60 PFU/cell; Tukey's HSD). At 4 hpi, free H1.2 was significantly increased ($P < 0.01$) to 115% ± 4% and 136% ± 8% in cells infected with 30 or 60 PFU/cell but not in cells infected with 10 PFU/cell (Table 4; Fig. 5A, n212). At 7 hpi, the increases in the pools of free H1.2 were no longer dependent on multiplicity ($P > 0.05$, Tukey's HSD). Free H1.2 was increased to 152% ± 9%, 145% ± 5%, or 161% ± 9% in cells infected with 10, 30, or 60 PFU/cell (Table 4; Fig. 5A, n212).

U2OS cells complement ICP0 mutations, such that n212 replicates with the same kinetics as wild-type HSV-1. As expected, therefore, H1.2 was mobilized in U2OS cells infected with n212 ($P < 0.01$) in a multiplicity-independent manner ($P > 0.05$ at 4 and 7 hpi; Tukey's HSD). At either multiplicity evaluated (10 or 30 PFU/cell), H1.2 T_{50} was reduced to 55% and further to 44% at 4 or 7 hpi, respectively (T_{50}, 5.2 ± 0.3 and 4.8 ± 0.4 s, respectively) (Table 6; Fig. 7, n212 U2OS). Low- and high-affinity chromatin binding were equally affected (T_{90} versus T_{50}; $P > 0.05$ for 10 and 30 PFU/cell at 4 hpi and 10

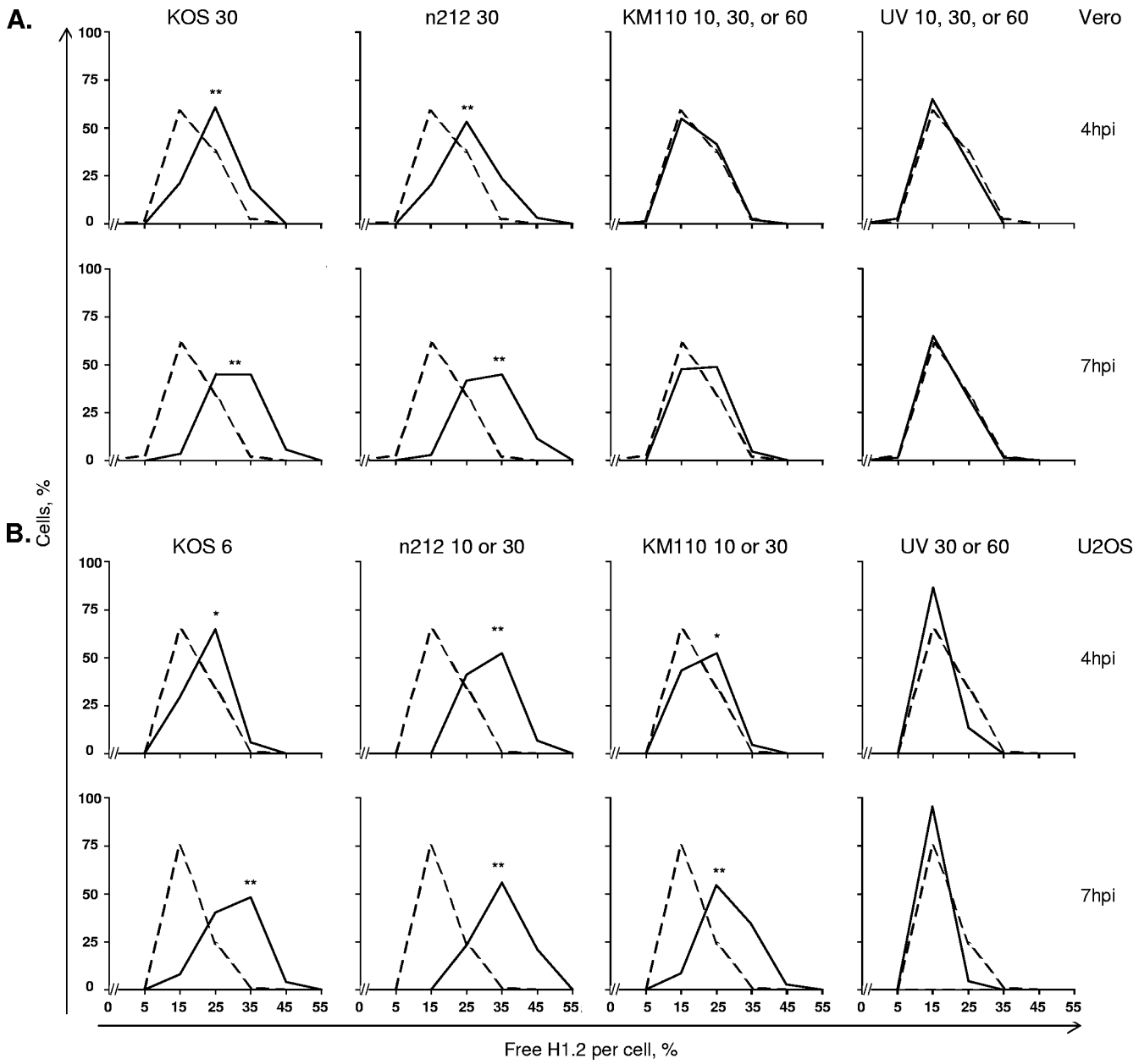

FIG. 5. The pool of free H1.2 increases during infection. Frequency distribution plot of the percentage of free H1.2 per individual cell. Vero (A) or U2OS (B) cells were transfected with plasmids expressing GFP-H1.2. Transfected cells were mock infected (dashed line) or infected (solid line) with the indicated multiplicity of HSV-1 strain KOS, n212, KM110, or UV-inactivated KOS. Free GFP-H1.2 was evaluated from 4 to 5 hpi (4 hpi) or 7 to 8 hpi (7 hpi) by FRAP ($n \geq 17$). **, $P < 0.01$; *, $P < 0.05$.

PFU/cell at 7 hpi; $P < 0.05$ for 30 PFU/cell at 7 hpi). As expected, the pools of free H1.2 were also significantly increased in a multiplicity-independent manner ($P > 0.05$ at 4 and 7 hpi, Tukey's HSD). Free H1.2 was increased to 152% ± 3% and 184% ± 4% at 4 and 7 hpi, respectively ($P < 0.01$) (Table 4; Fig. 5B, n212).

The degree of H1.2 mobilization and the increase in free H1.2 were dependent on multiplicity of infection under conditions in which expression of HSV-1 proteins and genome replication are also dependent on multiplicity. Therefore, HSV-1 transcription, specific HSV-1 proteins, or genome replication are involved in enhancing H1.2 mobilization and increasing the levels of free H1.2. Alternatively, enhanced H1.2 mobilization or an increase in free H1.2 may be required for HSV-1 transcription or DNA replication.

The enhanced mobilization of H1.2 and the increase in the levels of free H1.2 do not require HSV-1 DNA replication. We next evaluated H1.2 mobility under conditions in which HSV-1 DNA replication was inhibited. To this end, infected cells were treated with 400 μg/ml PAA to inhibit the HSV-1 DNA polymerase (47).

H1.2 was still significantly mobilized in Vero cells infected

TABLE 5. Nuclear ICP4 localization in cells infected with wild-type and mutant HSV-1 strains

Cell type	Virus strain	PFU/cell	Localization (avg ± SEM) at:					
			4 hpi			7 hpi		
			% Not detected	% Nuclear diffuse	% Replication compartment	% Not detected	% Nuclear diffuse	% Replication compartment
Vero	KOS	30	9 ± 2	40 ± 7	52 ± 8	13 ± 6	9 ± 4	78 ± 5
	n212	30	12 ± 1	78 ± 5	11 ± 5	7 ± 2	37 ± 10	56 ± 11
	KM110	30	94 ± 2	5 ± 2	1 ± 0	90 ± 2	10 ± 1	1 ± 1
	UV	30	100	0	0	100	0	0
U2OS	KOS	6	4 ± 1	19 ± 3	78 ± 4	6 ± 2	16 ± 5	79 ± 5
	n212	30	1 ± 1	10 ± 6	88 ± 6	0	1 ± 0	99 ± 0
	KM110	30	26 ± 10	47 ± 2	27 ± 12	11 ± 4	26 ± 6	63 ± 3
	UV	30	100	0	0	100	0	0

with KOS in the presence of PAA ($P < 0.01$). The H1.2 T_{50} was decreased to 34% of control at 7 hpi in Vero cells infected with 30 PFU/cell of KOS and treated with PAA (T_{50}, 7.4 ± 1.0 s) (Table 7; Fig. 8A, B, and C), the same degree as in the absence of PAA ($P > 0.05$) (Table 7; Fig. 8A and B). Also, as in the absence of PAA, H1.2 mobilization was the result of changes to low- and high-affinity chromatin binding (T_{90} versus T_{50}, $P > 0.05$ for 30 PFU/cell of KOS treated with PAA at 7 hpi) (Table 7). Moreover, there was still a net increase in the pool of free H1.2 ($P < 0.01$). Free H1.2 was increased to 161% ± 7% at 7 hpi in PAA-treated cells infected with 30 PFU/cell of KOS (Fig. 8D; Table 7), as in the cells not treated with PAA ($P > 0.05$). HSV-1 genome replication or strictly late HSV-1 proteins are therefore not required for the enhanced late mobilization of H1.2 or to increase its free pool.

Infecting virions with cross-linked genomes are not sufficient to mobilize H1.2. H1.2 was still mobilized to a basal level in Vero cells infected with KM110, although the vast majority of cells had little to no detectable ICP4 expression. Virion fusion with the host cell membrane or virion proteins (other than VP16 and ICP0) may therefore be sufficient to induce the basal mobilization of H1.2. We thus evaluated the mobilization of H1.2 in cells infected with UV-inactivated KOS, which fuses with the host cell and releases capsid and tegument proteins but expresses no HSV-1 genes. As expected, ICP4 expression was not detected in Vero or U2OS cells infected with 30 PFU/cell of UV-inactivated KOS (Table 5; Fig. 6, UV).

H1.2 was not mobilized at any time in either Vero or U2OS cells infected with UV-inactivated KOS, even at multiplicities of 60 PFU/cell ($P > 0.05$) (Tables 3 and 6; Fig. 7, UV). Furthermore, the pools of free H1.2 were not increased at any time in either Vero or U2OS cells infected with any multiplicity (10, 30, or 60 PFU/cell) (Table 4; Fig. 5A and B, UV). Viral fusion, capsid, and tegument proteins (other than VP16 or ICP0), or cross-linked HSV-1 genomes, were therefore not sufficient to induce H1.2 mobilization or to increase its free pool.

DISCUSSION

Here we have shown that linker histones are mobilized during HSV-1 infection. Mobilization of H1.2 resulted from changes to low- and high-affinity chromatin binding and led to a net increase in its free pool. H1.2 was mobilized to a basal degree under conditions of little to no HSV-1 gene expression (KM110 infection of Vero cells). However, mobilization was further increased above the basal degree and the pool of free H1.2 increased only if IE and E HSV-1 proteins were expressed. Such increases were independent of HSV-1 genome replication or L proteins.

Most current models propose that the naked infecting HSV-1 genome associates with histones during lytic infection (20, 33, 40). Such association would require synthesis of new histones or the movement of preexisting ones from domains containing cellular chromatin to those containing HSV-1 genomes (Fig. 1). The later depletion of histones from replication compartments (36, 50, 51) (Fig. 1) would subsequently require histone degradation or movement of histones away from the domains containing the HSV-1 genomes. Histone synthesis is tightly regulated at transcriptional and posttranscriptional levels. Most histones are synthesized only during S-phase (15, 21, 22, 32), whereas HSV-1 infects cells in any phase of the cell cycle and inhibits histone synthesis (55, 68). H3 levels consequently do not increase during HSV-1 infection (19, 23). It is therefore unlikely that the histones which bind to HSV-1 genomes are synthesized de novo in infected cells. Consistent with such a conclusion, we found that linker histones are instead mobilized during infection.

The observed mobility of each somatic H1 variant in mock-infected Vero cells was consistent with previous reports (62). Based on the average T_{50}, the H1 variants were classified into two groups. H1.4 and H1.5, which tend to associate with heterochromatin and have longer C-terminal domains, had significantly slower mobilities than $H1^0$, H1.1, H1.2, and H1.3, which tend to associate with euchromatin ($H1^0$, H1.1, H1.2, and H1.3) (62) or have shorter C-terminal domains ($H1^0$, H1.1, and H1.2) (62). Such consistency with previous results supports the suitability of our FRAP approach to evaluate H1 mobilization during HSV-1 infection.

Each of the somatic H1 variants except H1.4 was significantly mobilized during HSV-1 infection, although each was mobilized to a different degree and in differently sized subpopulations of cells. H1.2 was the most readily mobilized, whereas $H1^0$ was the least. H1.2 is also ubiquitously expressed, including in epithelial cells and fibroblasts (26, 44), and is therefore biologically relevant for lytic HSV-1 infections. $H1^0$,

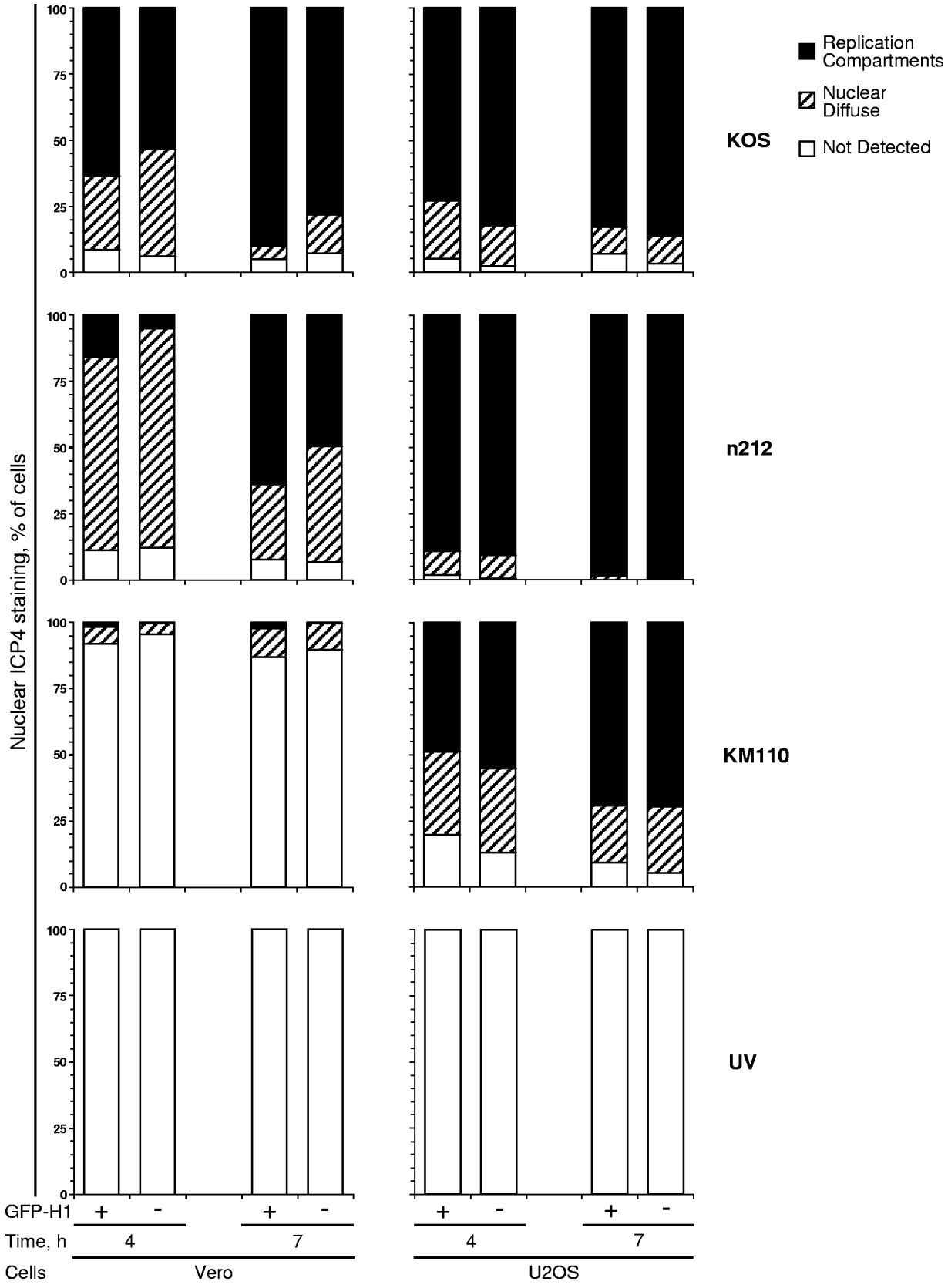

FIG. 6. ICP4 expression and accumulation into replication compartments in Vero or U2OS cells infected with wild-type or mutant HSV-1 strains. Bar graphs representing the percentage of HSV-1-infected cells transfected with GFP-H1.2 and expressing ICP4 as nuclear diffuse or accumulated into replication compartments. Vero or U2OS cells were transfected with plasmids expressing GFP-H1.2. Cells were infected with 30 PFU/cell of HSV-1 strain KOS, n212, KM110, or UV-inactivated KOS or with 6 PFU/cell of HSV-1 strain KOS (U2OS cells only). Cells were fixed at 4.5 (4) or 7.5 (7) hpi and stained for ICP4. Nuclear expression of ICP4 and accumulation into replication compartments in cells in which GFP-H1.2 was expressed (+) or not (−) were evaluated by fluorescence microscopy.

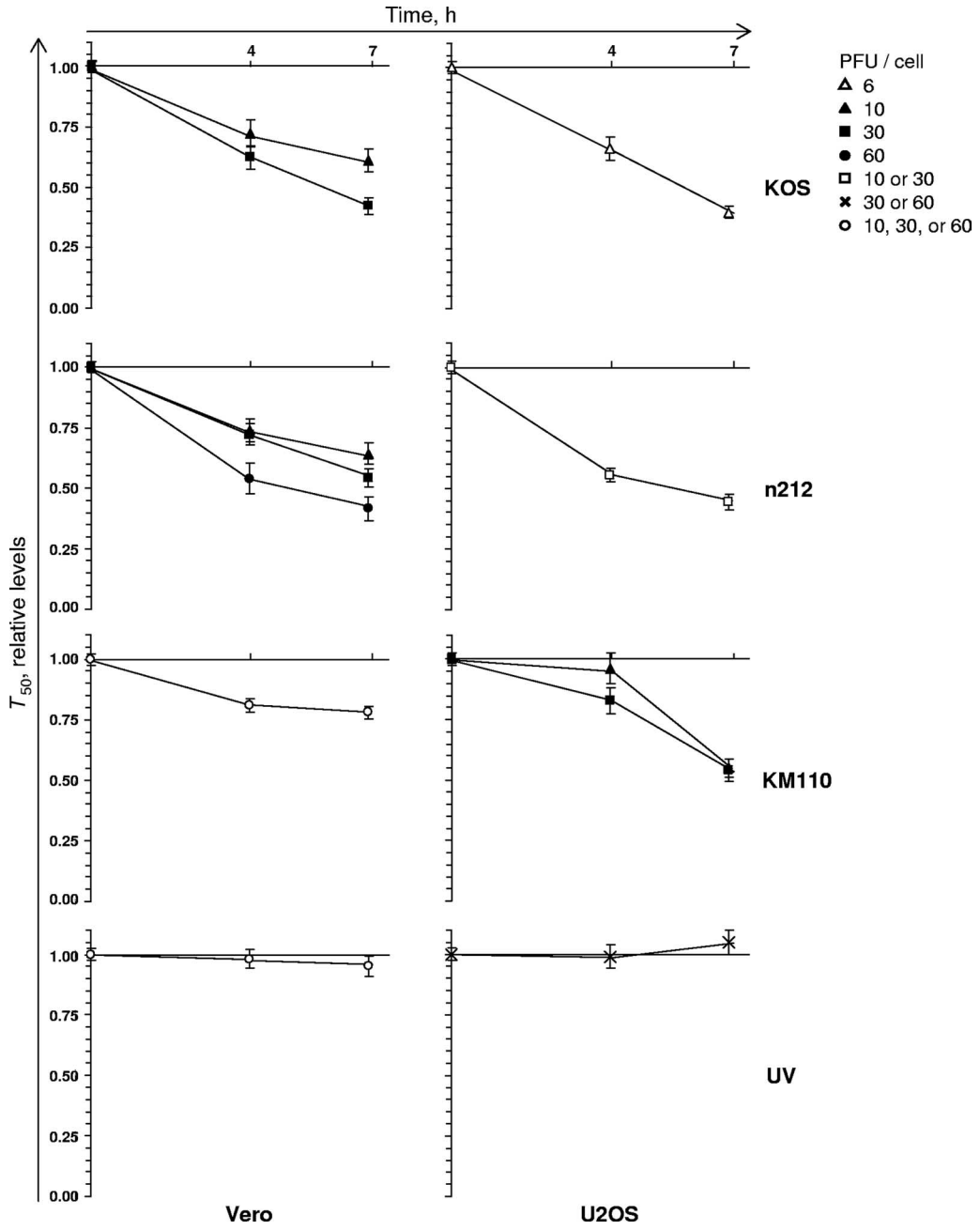

FIG. 7. Mobilization of H1.2 requires nuclear HSV-1 genomes but not ICP0 or VP16. Line graphs representing the average H1.2 T_{50} in HSV-1-infected cells normalized to mock-infected cells and plotted against time postinfection. Vero or U2OS cells were transfected with plasmids expressing GFP-H1.2. Transfected cells were mock infected or infected with 6, 10, 30, 60, 10 to 30, 30 to 60, or 10 to 60 PFU/cell of HSV-1 strain KOS, n212, KM110, or UV-inactivated KOS. Nuclear mobility of GFP-H1.2 was examined from 4 to 5 hpi (4) or 7 to 8 hpi (7) by FRAP. Error bars, standard errors of the means ($n \geq 25$), except for Vero KOS 10 at 4 and 7 hpi, Vero n212 60 at 4 and 7 hpi, U2OS KOS 6 at 4 hpi, U2OS KM110 10 at 4 and 7 hpi, and U2OS KM110 30 at 7 hpi ($n \geq 14$). Vero KOS data are a summary of the data presented in Fig. 4.

in contrast, is enriched in differentiated cells, such as neurons (26, 44). Its restricted mobilization may therefore be more relevant to latent infections.

The basal mobilization of H1.2 under conditions of little to no HSV-1 protein expression (Fig. 7; Table 3) was not due to virion fusion with the cell membrane or to proteins in the infecting virions (other than VP16 or ICP0). UV-inactivated HSV-1 did not induce it. Therefore, structural virion proteins or lipids are not sufficient to induce basal H1.2 mobilization, but nonstructural viral proteins are not required either. These results suggest that the basal mobilization of H1.2 is triggered by the presence of nuclear native (i.e., non-cross-linked) viral DNA.

KM110 did not induce the late enhancement of H1.2 mobilization in Vero cells, although it did so in U2OS cells, in which its replication was restored (Fig. 7). The lack of enhanced mobilization of H1.2 in KM110 infections of Vero cells may have resulted from the inhibition of transcription, or of expression of specific IE or E proteins. Conversely, the failure to

TABLE 6. Mobilization of H1.2 in U2OS cells infected with wild-type or mutant HSV-1 strains

Time (hpi)	Virus strain	PFU/cell	T_{50} (avg ± SEM)		% Cells with high H1 mobilization, T_{50}[a]	T_{90} (avg ± SEM)		% Cells with high H1 mobilization, T_{90}[b]
			Absolute (s)	Relative (%)		Absolute (s)	Relative (%)	
4			10.7 ± 0.4	100	16	88.6 ± 3.3	100	14
	KOS	6	8.0 ± 0.6	66 ± 5	76	64.7 ± 5.0	73 ± 7	53
	n212	10 or 30	5.2 ± 0.3	55 ± 3	84	55.1 ± 3.0	62 ± 4	52
	KM110	10	11.2 ± 0.9	96 ± 6	22	97.5 ± 8.6	110 ± 8	22
		30	7.7 ± 0.5	83 ± 5	38	66.4 ± 6.4	75 ± 8	42
	UV	30 or 60	11.8 ± 0.6	99 ± 5	22	93.9 ± 5.6	106 ± 6	24
7			12.4 ± 0.4	100	15	102.9 ± 3.7	100	16
	KOS	6	5.8 ± 0.4	40 ± 3	100	59.7 ± 5.1	58 ± 4	88
	n212	10 or 30	4.8 ± 0.4	44 ± 3	93	52.1 ± 4.9	51 ± 6	67
	KM110	10	6.8 ± 0.5	55 ± 4	88	58.6 ± 4.9	57 ± 5	75
		30	5.0 ± 0.4	54 ± 5	94	44.3 ± 6.5	43 ± 9	78
	UV	30 or 60	14.0 ± 0.6	105 ± 5	19	114.7 ± 5.9	111 ± 6	23

[a] Percentage of cells in which the T_{50} was >1 SD lower than the average T_{50} in mock-infected cells.
[b] Percentage of cells in which the T_{90} was >1 SD lower than the average T_{90} in mock-infected cells.

further mobilize H1.2 may have resulted in the inhibition of HSV-1 transcription and protein expression.

Approximately 40% of total nuclear H1.2 was in the free pool at 7 h after infection (Table 4, Vero 7 hpi KOS 30), when histone synthesis is inhibited (55, 57, 68). The increase in free H1.2 was therefore most likely from preexisting pools, such as those in cellular chromatin. H1 mobilization occurs through modulation of its binding to, and dissociation or displacement from, chromatin. Mobilization during infection may have resulted from promoting dissociation of H1.2 from chromatin, decreasing its affinity for chromatin binding, or competition for its binding sites. Posttranslational modifications (to H1 or core histones) and competition for binding sites both promote the dissociation of H1 from chromatin and decrease its rebinding affinity. Such modifications or competitions could therefore increase H1.2 free pools in infected cells.

In contrast to the mobilization during productive infection, basal mobilization of H1.2 during nonproductive infection did not result in an increase in its free pool (Fig. 5; compare KM110 in panels A and B). Under the latter conditions, H1.2 binding to chromatin was therefore altered such that there was an increased rate of exchange, but the rates of chromatin binding and dissociation or displacement were not altered relative to each other. HSV-1 proteins therefore alter the H1.2 chromatin exchange rates such that there is an increase in its free pool. Although H1.2 has not yet been directly shown to bind to HSV-1 genomes, it has a high affinity for naked DNA (60). If H1.2 did bind to HSV-1 genomes, then the passage of transcription complexes could displace bound H1.2, increasing its free pool. Viral proteins may also directly affect the interactions between histones and HSV-1 genomes. For example, VP16 recruits chromatin histone acetyltransferases and promotes removal of H3 from IE gene promoters (18, 34, 63). Both acetylation and removal of core histones promote dissociation of linker histone H1 from chromatin. VP16 may therefore inhibit binding of mobilized H1.2 to HSV-1 genomes. Consistent with such a model, free H1.2 did not increase in the absence of VP16 (and HSV-1 transcription) (Fig. 5A, KM110; Table 4). Also consistent with such a model, H1.2 was not mobilized by infection with UV-inactivated HSV-1 virions, and the VP16 in the input virions did therefore not induce an increase in free H1.2 (Fig. 5A and B, UV; Table 4, Vero and U2OS UV). Although VP16 was not essential to increase the level of free H1.2 in U2OS cells, the increase was still significantly greater in n212 than in KM110 infections (1.84- and 1.49-fold, respectively [Table 4]; $P < 0.01$). These strains only differ in the inactivation of VP16 in the latter. VP16 may therefore still contribute to the increase in free H1.2, even in U2OS cells.

TABLE 7. Mobilization of H1.2 in Vero cells infected with 30 PFU/cell of HSV-1 KOS and treated with PAA

Parameter	PAA	Mobilization (avg ± SEM)		% Cells with high H1 mobilization[a]
		Absolute (s)	Relative to mock-infected cells	
T_{50}	+	7.4 ± 1.0	0.34 ± 0.05	94*
	−	6.9 ± 0.5	0.42 ± 0.03	92*
T_{90}	+	67.4 ± 6.0	0.60 ± 0.04	94**
	−	65.0 ± 4.5	0.58 ± 0.05	74**
Free H1.2	+		1.61 ± 0.07	94***
	−		1.74 ± 0.06	92***

[a] *, percentage of cells in which the T_{50} was >1 SD lower than the average T_{50} in mock-infected cells; **, percentage of cells in which the T_{90} was >1 SD lower than the average T_{90} in mock-infected cells; ***, percentage of cells in which the level of free H1.2 was >1 SD above the average level of free H1.2 in mock-infected cells.

Productive HSV-1 infection activates the cellular DNA damage response (49, 64, 66), and H1.2 has been reported to translocate to the cytoplasm following double-strand breaks (24, 41). Mobilization of H1.2 during HSV-1 infection could therefore be the result of activation of DNA damage responses and subsequent release of H1.2. However, GFP-H1.2 fusion proteins were undetectable in the cytoplasm at any time postinfection (Fig. 1B). GFP-H1.2 was still strictly nuclear even at late times after infection in cells in which ICP4 was detected in the cytoplasm (Fig. 1B). Moreover, the late enhanced mobilization of H1.2 and the increase in its free pool was not affected by PAA, whereas only NBS1 has been reported activated during HSV-1 infection in the presence or absence of PAA (49, 65, 66). It is therefore unlikely that the mobilization of H1.2 dur-

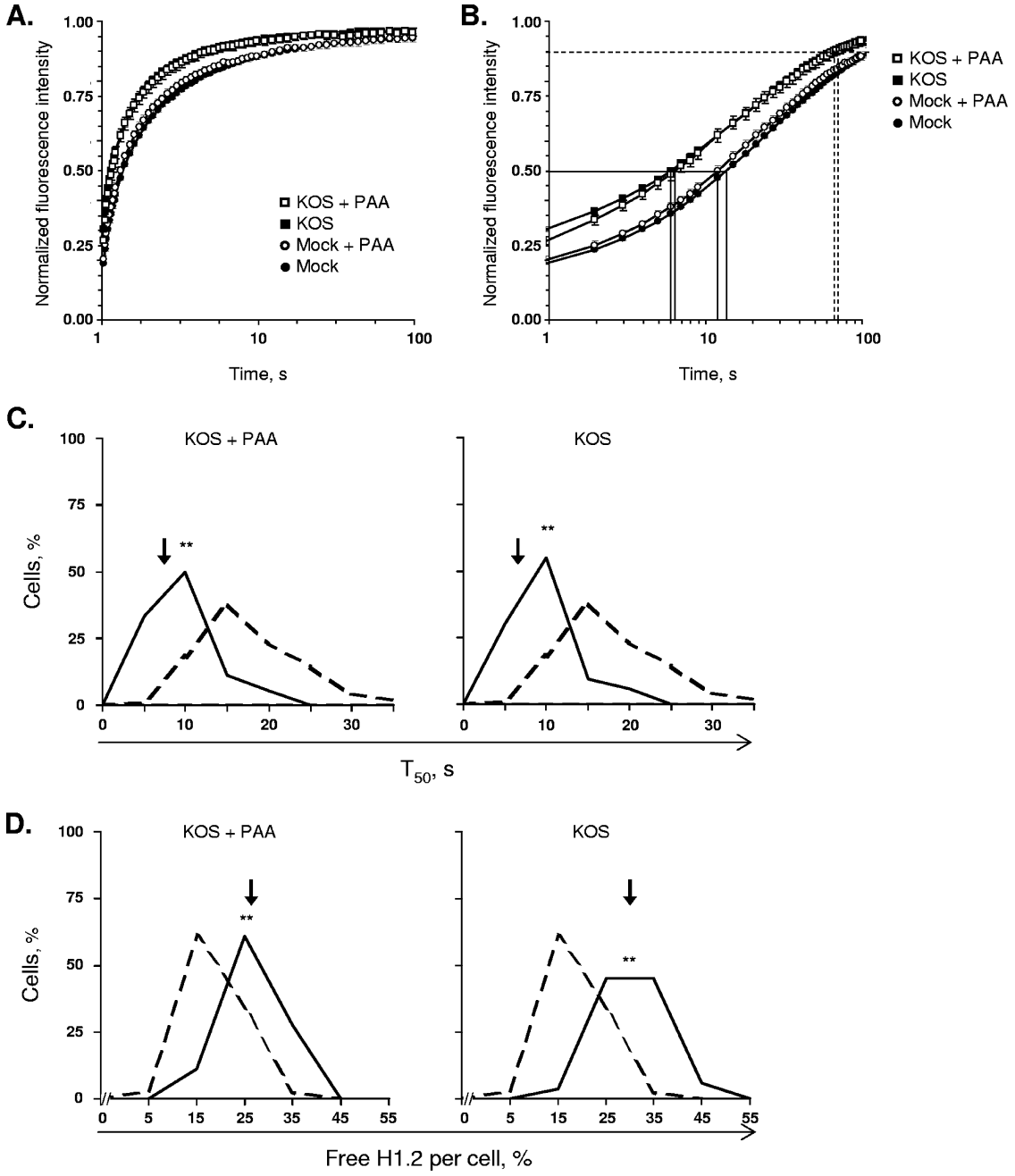

FIG. 8. Enhanced H1.2 mobilization or increased free H1.2 do not require HSV-1 genome replication. (A) Line graphs representing the normalized fluorescence intensity of the photobleached nuclear region over time. Vero cells were transfected with plasmids expressing GFP-H1.2, and mock infected or infected with 30 PFU/cell of HSV-1 strain KOS in the presence of 400 μg/ml of PAA or no drug (data from Fig. 4A were replotted for comparison). Nuclear mobility of GFP-H1.2 was examined from 7 to 8 hpi by FRAP. Error bars, standard errors of the means ($n \geq 18$); time is plotted on a linear scale. (B) The same data as in panel A, plotted on a semilogarithmic scale. Solid or dashed lines, times when 50 or 90% of the original relative fluorescence was recovered (T_{50} or T_{90}), respectively. Mock-infected cells had not recovered 90% of the original relative fluorescence when the measurements were stopped at 100 s. (C) Frequency distribution plot of the T_{50} per individual cell evaluated by FRAP as described for panel A. Dashed or solid lines, mock-infected or HSV-1 (30 PFU/cell strain KOS)-infected cells treated with 400 μg/ml of PAA or no drug (data from Fig. 4B were replotted for comparison). Arrows, mean T_{50} of the infected cell population. (D) Frequency distribution plot of the percentage of free H1.2 per individual cell evaluated by FRAP as described for panel A. Dashed or solid lines, mock-infected or HSV-1 (30 PFU/cell strain KOS)-infected cells treated with 400 μg/ml of PAA or no drug (data from Fig. 5A were replotted for comparison). Arrow, mean percentage of free H1.2 per cell of the infected cell population; **, $P < 0.01$.

ing HSV-1 infection is the result of activation of DNA damage responses.

The nuclear morphological changes during HSV-1 infection could have affected histone mobilization. The nuclear volume expands to up to twice its original size for approximately the first 10 hours of infection (36, 51). Viral replication compartments form and occupy additional volume during this expansion, but cellular chromatin is not yet

marginalized. H1 mobilization involves diffusion through the nucleoplasm to new potential binding sites. Changing the distance between binding sites would therefore affect H1.2 mobilization. If the increases in nuclear volume were greater than the volume occupied by replication compartments, then the relative distance between H1 binding sites would increase, and H1 would be mobilized because of the increased diffusion time between binding events. This hypothesis, however, is not well-supported by the kinetics of H1 diffusion, approximately 25 $\mu m^2 \cdot s^{-1}$, which is too fast to be affected by the relatively small changes in distance between binding sites in infected cells. Neither was this hypothesis supported by our experimental results. H1.2 mobilization did not correlate with the formation of replication compartments. Less than 2% of Vero cells infected with KM110 had replication compartments at early or late times postinfection, whereas 30 to 40% of them had a high degree of H1.2 mobilization. A similar trend was observed in infections with n212 at early times after infection. Whereas 44% of Vero cells had a high degree of H1.2 mobilization, and 35% a large increase in free H1.2, only 11% had replication compartments. Furthermore, replication compartments were formed in a similar percentage of Vero cells at late times postinfection with n212 as at early times postinfection with KOS (56% and 52%, respectively). However, a greater percentage of n212-infected cells had a high degree of H1.2 mobilization (83%) and large increase in free H1.2 (75%) at late times than KOS-infected cells at early times (61% and 52%, respectively). The altered nuclear morphology is therefore not a major contributing factor to H1.2 mobilization, although it may still affect it.

H1 binding to chromatin promotes the formation of higher-order, more compact structures, and cellular chromatin becomes marginalized late in infection, decreasing the distance between potential H1 binding sites. It is thus particularly surprising that H1.2 is further mobilized and the pool of free H1.2 is increased, precisely at these late times when chromatin is compacted.

The H1.2 T_{50} was decreased to almost less than half (42%) of that in mock-infected cells (Fig. 7, KOS Vero; Table 3). Such a degree of mobilization has previously been reported in cells treated with trichostatin A (TSA), a histone deacetylase inhibitor (70). TSA globally increases the levels of core histone acetylation, which in turn promote the dissociation of H1 from chromatin. $H1^0$-GFP and H1.1-GFP were mobilized in TSA-treated cells, such that their recovery of fluorescence occurred in 45 to 60% of the time required in untreated cells (35). However, H1 mobilization in HSV-1-infected cells is unlikely to be due to a global increase in core histone acetylation. Although the global levels of histone acetylation (of H3K9 and H3K14) are elevated up to 1.5-fold at 10 hpi, they are not changed (or perhaps even modestly decreased) at 4 and 7 hpi (23), when H1 is already significantly mobilized. Moreover, even though ICP0 inhibits histone deacetylases, such inhibition does not increase the global level of core histone acetylation (30), nor was ICP0 required for histone mobilization (Fig. 5A and B, n212; Fig. 7, n212).

Like acetylation of core histones, phosphorylation of H1 destabilizes its binding to chromatin and therefore results in its mobilization. The binding of H1.1 phospho-mimetic mutants to chromatin is destabilized such that their T_{50} is decreased up to 50% of wild type (17). Competition for H1-binding sites is yet another mechanism of H1 mobilization. HMG proteins compete for H1-binding sites and thus mobilize H1 (5, 6). Microinjection of different HMG proteins decreased the GFP-$H1^0$ T_{40} to 36 to 56% of control, depending on the specific HMG type (6). Interestingly, the transactivation activity of ICP4 is enhanced by binding to HMG A proteins (42). ICP4 may therefore induce changes to HMG function or nuclear localization, thereby affecting H1 mobilization. The specific mechanisms that contribute to H1 mobilization during HSV-1 infection are being investigated.

In summary, here we have shown that linker histones are mobilized in HSV-1-infected cells. The early mobilization requires nuclear native HSV-1 genomes but not expression of any HSV-1 proteins. The later enhanced mobilization of H1.2, and also the increase in its free pool, requires specific IE or E HSV-1 proteins or HSV-1 transcription, but not HSV-1 genome replication or L proteins. These histone mobilizations provide a mechanism for the early interactions between histones and infecting HSV-1 genomes and the later displacement of histones from HSV-1 replication compartments.

ACKNOWLEDGMENTS

This work was supported by operating grant MOP 49551 from the Canadian Institute for Health Research and 1006331 from the Burroughs Wellcome Fund. Our laboratory was equipped with funds provided by the Alberta Heritage Foundation for Medical Research (AHFMR) and the Faculty of Medicine. L.M.S. and M.J.H. are supported by Medical Scholar Awards from the AHFMR.

REFERENCES

1. **Arthur, J. L., C. G. Scarpini, V. Connor, R. H. Lachmann, A. M. Tolkovsky, and S. Efstathiou.** 2001. Herpes simplex virus type 1 promoter activity during latency establishment, maintenance, and reactivation in primary dorsal root neurons in vitro. J. Virol. **75:**3885–3895.
2. **Ascoli, C. A., and G. G. Maul.** 1991. Identification of a novel nuclear domain. J. Cell Biol. **112:**785–795.
3. **Cai, W., and P. A. Schaffer.** 1992. Herpes simplex virus type 1 ICP0 regulates expression of immediate-early, early, and late genes in productively infected cells. J. Virol. **66:**2904–2915.
4. **Cai, W. Z., and P. A. Schaffer.** 1989. Herpes simplex virus type 1 ICP0 plays a critical role in the de novo synthesis of infectious virus following transfection of viral DNA. J. Virol. **63:**4579–4589.
5. **Catez, F., D. T. Brown, T. Misteli, and M. Bustin.** 2002. Competition between histone H1 and HMGN proteins for chromatin binding sites. EMBO Rep. **3:**760–766.
6. **Catez, F., H. Yang, K. J. Tracey, R. Reeves, T. Misteli, and M. Bustin.** 2004. Network of dynamic interactions between histone H1 and high-mobility-group proteins in chromatin. Mol. Cell. Biol. **24:**4321–4328.
7. **Coleman, H. M., V. Connor, Z. S. Cheng, F. Grey, C. M. Preston, and S. Efstathiou.** 2008. Histone modifications associated with herpes simplex virus type 1 genomes during quiescence and following ICP0-mediated de-repression. J. Gen. Virol. **89:**68–77.
8. **Deshmane, S. L., and N. W. Fraser.** 1989. During latency, herpes simplex virus type 1 DNA is associated with nucleosomes in a chromatin structure. J. Virol. **63:**943–947.
9. **Doenecke, D., W. Albig, H. Bouterfa, and B. Drabent.** 1994. Organization and expression of H1 histone and H1 replacement histone genes. J. Cell. Biochem. **54:**423–431.
10. **Everett, R. D.** 1984. Trans activation of transcription by herpes virus products: requirement for two HSV-1 immediate-early polypeptides for maximum activity. EMBO J. **3:**3135–3141.
11. **Everett, R. D., W. C. Earnshaw, J. Findlay, and P. Lomonte.** 1999. Specific destruction of kinetochore protein CENP-C and disruption of cell division by herpes simplex virus immediate-early protein Vmw110. EMBO J. **18:**1526–1538.
12. **Everett, R. D., J. Murray, A. Orr, and C. M. Preston.** 2007. Herpes simplex virus type 1 genomes are associated with ND10 nuclear substructures in quiescently infected human fibroblasts. J. Virol. **81:**10991–11004.
13. **Gu, H., Y. Liang, G. Mandel, and B. Roizman.** 2005. Components of the

REST/CoREST/histone deacetylase repressor complex are disrupted, modified, and translocated in HSV-1-infected cells. Proc. Natl. Acad. Sci. USA **102:**7571–7576.
14. **Gu, H., and B. Roizman.** 2007. Herpes simplex virus-infected cell protein 0 blocks the silencing of viral DNA by dissociating histone deacetylases from the CoREST-REST complex. Proc. Natl. Acad. Sci. USA **104:**17134–17139.
15. **Gunjan, A., J. Paik, and A. Verreault.** 2005. Regulation of histone synthesis and nucleosome assembly. Biochimie **87:**625–635.
16. **Harris, R. A., and C. M. Preston.** 1991. Establishment of latency in vitro by the herpes simplex virus type 1 mutant in1814. J. Gen. Virol. **72:**907–913.
17. **Hendzel, M. J., M. A. Lever, E. Crawford, and J. P. Th'ng.** 2004. The C-terminal domain is the primary determinant of histone H1 binding to chromatin in vivo. J. Biol. Chem. **279:**20028–20034.
18. **Herrera, F. J., and S. J. Triezenberg.** 2004. VP16-dependent association of chromatin-modifying coactivators and underrepresentation of histones at immediate-early gene promoters during herpes simplex virus infection. J. Virol. **78:**9689–9696.
19. **Huang, J., J. R. Kent, B. Placek, K. A. Whelan, C. M. Hollow, P. Y. Zeng, N. W. Fraser, and S. L. Berger.** 2006. Trimethylation of histone H3 lysine 4 by Set1 in the lytic infection of human herpes simplex virus 1. J. Virol. **80:**5740–5746.
20. **Ishov, A. M., and G. G. Maul.** 1996. The periphery of nuclear domain 10 (ND10) as site of DNA virus deposition. J. Cell Biol. **134:**815–826.
21. **Jaeger, S., S. Barends, R. Giege, G. Eriani, and F. Martin.** 2005. Expression of metazoan replication-dependent histone genes. Biochimie **87:**827–834.
22. **Kamakaka, R. T., and S. Biggins.** 2005. Histone variants: deviants? Genes Dev. **19:**295–310.
23. **Kent, J. R., P. Y. Zeng, D. Atanasiu, J. Gardner, N. W. Fraser, and S. L. Berger.** 2004. During lytic infection herpes simplex virus type 1 is associated with histones bearing modifications that correlate with active transcription. J. Virol. **78:**10178–10186.
24. **Konishi, A., S. Shimizu, J. Hirota, T. Takao, Y. Fan, Y. Matsuoka, L. Zhang, Y. Yoneda, Y. Fujii, A. I. Skoultchi, and Y. Tsujimoto.** 2003. Involvement of histone H1.2 in apoptosis induced by DNA double-strand breaks. Cell **114:**673–688.
25. **Leinbach, S. S., and W. C. Summers.** 1980. The structure of herpes simplex virus type 1 DNA as probed by micrococcal nuclease digestion. J. Gen. Virol. **51:**45–59.
26. **Lennox, R. W., and L. H. Cohen.** 1983. The histone H1 complements of dividing and nondividing cells of the mouse. J. Biol. Chem. **258:**262–268.
27. **Lever, M. A., J. P. Th'ng, X. Sun, and M. J. Hendzel.** 2000. Rapid exchange of histone H1.1 on chromatin in living human cells. Nature **408:**873–876.
28. **Lomonte, P., and E. Morency.** 2007. Centromeric protein CENP-B proteasomal degradation induced by the viral protein ICP0. FEBS Lett. **581:**658–662.
29. **Lomonte, P., K. F. Sullivan, and R. D. Everett.** 2001. Degradation of nucleosome-associated centromeric histone H3-like protein CENP-A induced by herpes simplex virus type 1 protein ICP0. J. Biol. Chem. **276:**5829–5835.
30. **Lomonte, P., J. Thomas, P. Texier, C. Caron, S. Khochbin, and A. L. Epstein.** 2004. Functional interaction between class II histone deacetylases and ICP0 of herpes simplex virus type 1. J. Virol. **78:**6744–6757.
31. **Lukonis, C. J., J. Burkham, and S. K. Weller.** 1997. Herpes simplex virus type 1 prereplicative sites are a heterogeneous population: only a subset are likely to be precursors to replication compartments. J. Virol. **71:**4771–4781.
32. **Marzluff, W. F., and R. J. Duronio.** 2002. Histone mRNA expression: multiple levels of cell cycle regulation and important developmental consequences. Curr. Opin. Cell Biol. **14:**692–699.
33. **Maul, G. G., A. M. Ishov, and R. D. Everett.** 1996. Nuclear domain 10 as preexisting potential replication start sites of herpes simplex virus type-1. Virology **217:**67–75.
34. **Memedula, S., and A. S. Belmont.** 2003. Sequential recruitment of HAT and SWI/SNF components to condensed chromatin by VP16. Curr. Biol. **13:**241–246.
35. **Misteli, T., A. Gunjan, R. Hock, M. Bustin, and D. T. Brown.** 2000. Dynamic binding of histone H1 to chromatin in living cells. Nature **408:**877–881.
36. **Monier, K., J. C. Armas, S. Etteldorf, P. Ghazal, and K. F. Sullivan.** 2000. Annexation of the interchromosomal space during viral infection. Nat. Cell Biol. **2:**661–665.
37. **Mossman, K. L., and J. R. Smiley.** 1999. Truncation of the C-terminal acidic transcriptional activation domain of herpes simplex virus VP16 renders expression of the immediate-early genes almost entirely dependent on ICP0. J. Virol. **73:**9726–9733.
38. **Mouttet, M. E., D. Guetard, and J. M. Bechet.** 1979. Random cleavage of intranuclear herpes simplex virus DNA by micrococcal nuclease. FEBS Lett. **100:**107–109.
39. **Muggeridge, M. I., and N. W. Fraser.** 1986. Chromosomal organization of the herpes simplex virus genome during acute infection of the mouse central nervous system. J. Virol. **59:**764–767.
40. **Oh, J., and N. W. Fraser.** 2007. Temporal association of the herpes simplex virus genome with histone proteins during a lytic infection. J. Virol. **82:**3530–3537.
41. **Okamura, H., K. Yoshida, B. R. Amorim, and T. Haneji.** 2008. Histone H1.2 is translocated to mitochondria and associates with Bak in bleomycin-induced apoptotic cells. J. Cell Biochem. **103:**1488–1496.
42. **Panagiotidis, C. A., and S. J. Silverstein.** 1999. The host-cell architectural protein HMG I(Y) modulates binding of herpes simplex virus type 1 ICP4 to its cognate promoter. Virology **256:**64–74.
43. **Parseghian, M. H., A. H. Henschen, K. G. Krieglstein, and B. A. Hamkalo.** 1994. A proposal for a coherent mammalian histone H1 nomenclature correlated with amino acid sequences. Protein Sci. **3:**575–587.
44. **Pehrson, J. R., and R. D. Cole.** 1982. Histone H1 subfractions and H10 turnover at different rates in nondividing cells. Biochemistry **21:**456–460.
45. **Preston, C. M., and M. J. Nicholl.** 1997. Repression of gene expression upon infection of cells with herpes simplex virus type 1 mutants impaired for immediate-early protein synthesis. J. Virol. **71:**7807–7813.
46. **Samaniego, L. A., L. Neiderhiser, and N. A. DeLuca.** 1998. Persistence and expression of the herpes simplex virus genome in the absence of immediate-early proteins. J. Virol. **72:**3307–3320.
47. **Schang, L. M., A. Rosenberg, and P. A. Schaffer.** 2000. Roscovitine, a specific inhibitor of cellular cyclin-dependent kinases, inhibits herpes simplex virus DNA synthesis in the presence of viral early proteins. J. Virol. **74:**2107–2120.
48. **Seyedin, S. M., and W. S. Kistler.** 1979. H1 histone subfractions of mammalian testes. 1. Organ specificity in the rat. Biochemistry **18:**1371–1375.
49. **Shirata, N., A. Kudoh, T. Daikoku, Y. Tatsumi, M. Fujita, T. Kiyono, Y. Sugaya, H. Isomura, K. Ishizaki, and T. Tsurumi.** 2005. Activation of ataxia telangiectasia-mutated DNA damage checkpoint signal transduction elicited by herpes simplex virus infection. J. Biol. Chem. **280:**30336–30341.
50. **Simpson-Holley, M., J. Baines, R. Roller, and D. M. Knipe.** 2004. Herpes simplex virus 1 U_L31 and U_L34 gene products promote the late maturation of viral replication compartments to the nuclear periphery. J. Virol. **78:**5591–5600.
51. **Simpson-Holley, M., R. C. Colgrove, G. Nalepa, J. W. Harper, and D. M. Knipe.** 2005. Identification and functional evaluation of cellular and viral factors involved in the alteration of nuclear architecture during herpes simplex virus 1 infection. J. Virol. **79:**12840–12851.
52. **Smibert, C. A., and J. R. Smiley.** 1990. Differential regulation of endogenous and transduced beta-globin genes during infection of erythroid cells with a herpes simplex virus type 1 recombinant. J. Virol. **64:**3882–3894.
53. **Smiley, J. R., C. Smibert, and R. D. Everett.** 1987. Expression of a cellular gene cloned in herpes simplex virus: rabbit beta-globin is regulated as an early viral gene in infected fibroblasts. J. Virol. **61:**2368–2377.
54. **Smith, K. O.** 1964. Relationship between the envelope and the infectivity of herpes simplex virus. Proc. Soc. Exp. Biol. Med. **115:**814–816.
55. **Sorenson, C. M., P. A. Hart, and J. Ross.** 1991. Analysis of herpes simplex virus-induced mRNA destabilizing activity using an in vitro mRNA decay system. Nucleic Acids Res. **19:**4459–4465.
56. **Sourvinos, G., and R. D. Everett.** 2002. Visualization of parental HSV-1 genomes and replication compartments in association with ND10 in live infected cells. EMBO J. **21:**4989–4997.
57. **Spencer, C. A., M. E. Dahmus, and S. A. Rice.** 1997. Repression of host RNA polymerase II transcription by herpes simplex virus type 1. J. Virol. **71:**2031–2040.
58. **Spencer, C. A., M. J. Kruhlak, H. L. Jenkins, X. Sun, and D. P. Bazett-Jones.** 2000. Mitotic transcription repression in vivo in the absence of nucleosomal chromatin condensation. J. Cell Biol. **150:**13–26.
59. **Stevens, J. G., E. K. Wagner, G. B. Devi-Rao, M. L. Cook, and L. T. Feldman.** 1987. RNA complementary to a herpesvirus alpha gene mRNA is prominent in latently infected neurons. Science **235:**1056–1059.
60. **Talasz, H., N. Sapojnikova, W. Helliger, H. Lindner, and B. Puschendorf.** 1998. In vitro binding of H1 histone subtypes to nucleosomal organized mouse mammary tumor virus long terminal repeat promotor. J. Biol. Chem. **273:**32236–32243.
61. **Taylor, T. J., E. E. McNamee, C. Day, and D. M. Knipe.** 2003. Herpes simplex virus replication compartments can form by coalescence of smaller compartments. Virology **309:**232–247.
62. **Th'ng, J. P., R. Sung, M. Ye, and M. J. Hendzel.** 2005. H1 family histones in the nucleus. Control of binding and localization by the C-terminal domain. J. Biol. Chem. **280:**27809–27814.
63. **Tumbar, T., G. Sudlow, and A. S. Belmont.** 1999. Large-scale chromatin unfolding and remodeling induced by VP16 acidic activation domain. J. Cell Biol. **145:**1341–1354.
64. **Wilkinson, D. E., and S. K. Weller.** 2006. Herpes simplex virus type I disrupts the ATR-dependent DNA-damage response during lytic infection. J. Cell Sci. **119:**2695–2703.
65. **Wilkinson, D. E., and S. K. Weller.** 2005. Inhibition of the herpes simplex virus type 1 DNA polymerase induces hyperphosphorylation of replication protein A and its accumulation at S-phase-specific sites of DNA damage during infection. J. Virol. **79:**7162–7171.
66. **Wilkinson, D. E., and S. K. Weller.** 2004. Recruitment of cellular recombination and repair proteins to sites of herpes simplex virus type 1 DNA replication is dependent on the composition of viral proteins within prereplicative sites and correlates with the induction of the DNA damage response. J. Virol. **78:**4783–4796.

67. **Wysocka, J., M. P. Myers, C. D. Laherty, R. N. Eisenman, and W. Herr.** 2003. Human Sin3 deacetylase and trithorax-related Set1/Ash2 histone H3-K4 methyltransferase are tethered together selectively by the cell-proliferation factor HCF-1. Genes Dev. **17:**896–911.
68. **Yager, D. R., and S. L. Bachenheimer.** 1988. Synthesis and metabolism of cellular transcripts in HSV-1 infected cells. Virus Genes **1:**135–148.
69. **Yao, F., and P. A. Schaffer.** 1995. An activity specified by the osteosarcoma line U2OS can substitute functionally for ICP0, a major regulatory protein of herpes simplex virus type 1. J. Virol. **69:**6249–6258.
70. **Yoshida, M., M. Kijima, M. Akita, and T. Beppu.** 1990. Potent and specific inhibition of mammalian histone deacetylase both in vivo and in vitro by trichostatin A. J. Biol. Chem. **265:**17174–17179.